mRNA turnover and translational control. Considering the important cellular functions of YB-1, it is possible that its expression is highly regulated in eukaryotes. In fact, the YB-1 gene behaves like a primary response gene. Stimulation of mammalian cell proliferation in culture or *in vivo* results in increased YB-1 synthesis. The cellular level of YB-1 is usually controlled by regulating the translation of its mRNA. It is thought that an increase in the cellular YB-1 concentration could alter the translation and stability of some mRNAs. Therefore, several pathways exist to control the function of this important cellular protein.

The 5′- and 3′-untranslated regions (UTRs) of eukaryotic mRNAs are known to play a crucial role in post-transcriptional regulation that modulates nucleo-cytoplasmic mRNA transport, translation efficiency, subcellular localization and stability (19). Several regulatory signals have already been identified within the 5′- or 3′-UTR sequences (20). These signals tend to correspond to short oligonucleotide tracts, able to fold into specific secondary structures which provide binding sites for various regulatory proteins (21–23).

To examine how YB-1 mRNA translation is regulated in eukaryotic cells, we examined the possible role of its relatively long 5′-UTR. Deletion of the YB-1 mRNA 5′-UTR enhances translational activity in both *in vitro* and *in vivo* systems. The affinities of YB-1 for 5′-UTR probe sequences of various lengths were evaluated by RNA gel shift assays; the affinity of YB-1 was higher for the full-length 5′-UTR than for truncated sequences. The addition of recombinant YB-1 inhibited translation through the 5′-UTR of its mRNA; this effect was particularly marked when the full-length 5′-UTR was used. In this study, we have demonstrated for the first time that the 5′-UTR region of human YB-1 mRNA plays an important role in determining the conditions of YB-1 biosynthesis at the translational level.

MATERIALS AND METHODS

Construction of fusion protein expression plasmids

The plasmids containing full-length glutathione *S*-transferase (GST)–YB-1 cDNA fusions, GST–YB-1 deletion mutants and Flag–YB-1 were described previously (24–26).

Reporter gene constructs

A pT7 control plasmid, for *in vitro* transcription and translation experiments, was constructed by digesting luciferase cDNA of a pGL3 basic vector (Promega, Madison, WI) with EcoRI, blunting with Klenow enzyme, and ligation to pT7Blue3 (Novagen, Madison, WI). The pT7-YB5′-1 plasmid was constructed as follows. The entire length of the YB-1 5′-UTR was amplified by PCR from human YB-1 cDNA. The forward primer was 5′-AGGCAGGAACGGTTGTAGGT-3′ and the reverse primer was 5′-gtttttggcgtcttccat-GGTTGCGGTGATGG-3′. The latter contains a luciferase coding sequence at the 5′-end (shown in lower case). A luciferase cDNA fragment was also amplified by PCR from a pGL3 basic vector, using the forward primer 5′-CCATCACCGCAACCatggaagacgccaaaaac-3′, complementary to the reverse primer of the YB-1 5′-UTR and the reverse primer 5′-ttacacggcgatctttcc-3′. Each PCR-amplified fragment was ligated with the complementary primer regions and amplified by PCR using the complementary primer pair. The YB-1 5′-UTR-ligated luciferase cDNA fragment was cloned into the EcoRI-digested pT7Blue3 vector in order to generate plasmid pT7-YB5′-1. To functionally characterize the 5′-UTR of the human YB-1 gene, a series of 5′-deletion plasmids (pT7-YB5′-2–pT7-YB5′-6) were amplified by PCR using the pT7-YB5′-1 plasmid as a template. The forward primers were 5′-AAGGTCCAATGAGAATGGAGGA-3′ (pT7-YB5′-2), 5′-AAGCTAGGGATTGGGGTCAG-3′ (pT7-YB5′-3), 5′-CCT-AGGGCGGGTCGCTCGTA-3′ (pT7-YB5′-4), 5′-CGATCG-GTAGCGGGAGCGGAG-3′ (pT7-YB5′-5) and 5′-CCG-CCGCCGCCGGCC-3′ (pT7-YB5′-6). Each of the PCR-amplified fragments were cloned into the EcoRI-digested pT7Blue3 vector to generate the pT7-YB5′-2–pT7-YB5′-6 plasmids. To construct pCMV and pCMV-YB5′-1–pCMV-YB5′-6 plasmids suitable for expression in mammalian cells, the pT7 or pT7-YB5′-1–pT7-YB5′-6 plasmids were digested with EcoRI. The fragments of luciferase cDNA were ligated into the EcoRI-digested pIRES-EYFP vector (Clontech, Palo Alto, CA), using various sizes of the YB-1 5′-UTR region (pCMV-YB5′-1–pCMV-YB5′-6); a non-ligated fragment (pCMV) was used as a control.

Site-directed mutagenesis of the YB-1 5′-UTR in pT7-YB5′-1 was performed using a PCR-based method. To obtain pT7-YBM1–pT7-YBM3, the full length of the YB-1 5′-UTR sequence was first amplified by PCR. The forward primers were 5′-GGTGGGCAGTACATCAGTACCACTGG-3′ (pT7-YBM1), 5′-GCGGGTCGCTAGAGAGGCTTATCCCGC-3′ (pT7-YBM2), 5′-CATTCTCGCTAGAACAGTCGGTAG-CGGG-3′ (pT7-YBM3) and the reverse primers were 5′-CCAGTGGTACTGATGTACTGCCCACC-3′ (pT7-YBM1), 5′GCGGGATAAGCCTCTCTAGCGACCCGC-3′ (pT7-YBM2) and 5′-CCCGCTACCGACTGTTCTAGCGAGA-ATG-3′ (pT7-YBM3). A second PCR was then performed with Taq polymerase using the first PCR products as templates. The PCR products were cloned into the EcoRI-digested pT7Blue3 vector in order to generate the pT7-YBM1–pT7-YBM3 plasmids. All constructs were confirmed by sequencing using a DNA sequencing system (model 377; Applied Biosystems, Foster City, CA).

Cell lines

A human epidermoid cancer cell line, KB3-1, was cultured in MEM supplemented with 10% newborn calf serum. The human lung cancer cell line H1299 was cultured in RPMI supplemented with 10% fetal bovine serum (FBS). HUVECs were isolated from individual human umbilical cord veins by collagenase digestion and were routinely cultured on type I collagen-coated plates in endothelial cell growth medium (Clonetics, Boston, MA) supplemented with 2% FBS. Tissue samples were obtained under an Institutional Review Board approved protocol, after the subjects had provided informed consent. The cells were maintained under standard cell culture conditions at 37°C and 5% CO_2 in a humid environment.

Recombinant proteins and antibodies

Recombinant proteins were expressed in *Escherichia coli* DH5α. YB-1 and YB-1 deletion mutants were purified as GST fusion proteins as described previously (25). Briefly, GST fusion protein expressed in bacteria was induced by incubation with isopropyl-1-thio-β-D-galactopyranoside and cells were

lysed by sonication in 1 ml of binding buffer [1 mM ditiothreitol, 0.5 mM phenylmethylsulfonyl fluoride (PMSF), 200 mM NaCl, 10% v/v glycerol, 1% Triton-X, in phosphate-buffered saline (PBS) pH 7.3]. Cellular debris was removed by centrifugation and the supernatants were subjected to affinity column chromatography using glutathione–Sepharose 4B (Amersham Biosciences, Piscataway, NJ) according to the manufacturer's recommendations. Antibody to YB-1 was generated as described previously (27).

Primer extension by reverse transcriptase

The primer extension experiments were carried out as described previously (28). Total RNA was prepared from each cell line using an RNeasy Miniprep Kit (Qiagen, Chatsworth, CA) and a QIAshredder microspin homogenizer according to the manufacturer's recommendations. The poly(A)$^+$ RNA was isolated from the total RNA using a Poly(A)$^+$ Isolation Kit from Total RNA (Nippon Gene Co. Ltd, Tokyo, Japan). The primer for the primer extension analysis, 5′-GCTCATGGTTGCGGTGATGG-3′, was synthesized to hybridize the sense strand between nucleotides −14 and +6 in the first exon of the YB-1 gene. The synthetic primer was labeled at its 5′-end with [γ-^{32}P]ATP using T4 polynucleotide kinase and hybridized to 1 μg poly(A)$^+$ RNA in 80% formamide, 0.4 M NaCl, 40 mM PIPES (pH 6.4) and 1 mM EDTA for 4 h at 50°C. After precipitation, the nucleic acid pellet was dissolved in reverse transcriptase buffer (Invitrogen Corp., Carlsbad, CA). The primer was extended with 200 U of SuperScript II RNase H$^-$ reverse transcriptase (Invitrogen) using 1 mM each of the four deoxynucleotides. After 1 h at 37°C, the reaction was neutralized and the DNA was collected. The reaction products were analyzed on a 7 M urea–8% polyacrylamide gel to determine the size of the extended product. The gel was exposed to an imaging plate and the blots were visualized and quantified using a phosphorimaging analyzer (model BAS 2000; Fuji Photo Film Co., Tokyo, Japan) and the Image Gauge (version 3.4) program.

RNA immunoprecipitation assay

Cells (100 mm dishes) were transfected with 5 μg of Flag–YB-1 plasmid DNA using LipofectAMINE 2000 reagent (Invitrogen). After 48 h, the cell extract was preincubated with protein A/G–agarose in TNE buffer [50 mM Tris–HCl (pH 7.5), 150 mM NaCl, 1 mM EDTA, 0.5% Nonidet P-40, 1 mM PMSF, 10 μg/ml leupeptin, 10 μg/ml aprotinin] for 1 h at 4°C with rotation. After centrifugation, the supernatant was incubated with anti-Flag M2-agarose affinity gel (Sigma Chemical Co., St Louis, MO) for 12 h at 4°C with rotation in TNE buffer. The beads were washed four times with TNE buffer. After centrifugation, total RNA was extracted from the precipitate using a RNeasy Miniprep Kit (Qiagen). Total mRNAs were reverse transcribed and amplified by PCR using the ThermoScript RT–PCR System (Invitrogen). The following YB-1- and β-actin-specific primer pairs were used: the forward primers were 5′-ACCACAGTATTCCAACCCTCCTG-3′ (YB-1) and 5′-CTGGCACCACACCTTCTACAATG-3′ (β-actin) and the reverse primers were 5′-ATCTTCTTCATTGCCGTCCTCTC-3′ (YB-1) and 5′-ATAGCAACGTACATGGCTGGGG-3′ (β-actin). The RT–PCR amplification products were analyzed by 2% agarose gel electrophoresis.

RNA band shift assays

The RNA electrophoretic mobility shift assay (REMSA) was carried out according to established techniques (29). Briefly, ^{32}P-labeled YB-1 5′-UTR probe was transcribed *in vitro* from the plasmid pT7blue3, which contains a sequence corresponding to the 5′-UTR of YB-1. An aliquot of 2 μg of the linearized plasmid was transcribed *in vitro* by T7 RNA polymerase in the presence of [α-^{32}P]UTP. The DNA template was removed by digestion with DNase I and the YB-1 5′-UTR probe was then extracted by column chromatography. To form RNA–protein complexes, 1–10 μg of cytoplasmic protein or the indicated amount of purified GST–YB-1 was incubated with ^{32}P-labeled YB-1 5′-UTR probe at 25°C for 15 min. Next, the samples underwent electrophoresis through a 4% non-denaturing polyacrylamide gel (polyacrylamide:bisacrylamide, 80:1) in Tris–borate buffer. For the supershift experiments, 2 μg of the YB-1 antibody was incubated with cytoplasmic protein or purified GST–YB-1 at 25°C for 5 min before adding the ^{32}P-labeled YB-1 5′-UTR probe. The gels were dried, visualized and then quantified as described above for the primer extension analysis.

In vitro transcription and translation

An aliquot of 2 μg of plasmid pT7Blue3, which encodes both luciferase cDNA ligated to the YB-1 mRNA 5′-UTR region (YB-1 5′-UTR–luciferase) as well as luciferase cDNA not ligated to the YB-1 mRNA 5′-UTR region (luciferase) (see Fig. 2A), was transcribed *in vitro* using an *In vitro* Transcription System (Promega). The DNA template was removed by digestion with DNase I and the RNA was purified by phenol/chloroform extraction. The integrity of the RNA was then examined using an Agilent 2000 Bioanalizer (Yokogawa, Osaka, Japan). Then, 50 ng of each RNA was translated using a rabbit reticulocyte lysate system (Promega). The luciferase assay was performed after incubation for 1.5 h at 30°C as described previously (18). To characterize the translation inhibition of each of the reporter constructs, the indicated amounts of GST fusion proteins were added to the rabbit reticulocyte lysate system either initially or after 10 min of incubation using 50 ng of the RNA constructs. The *in vitro* translation was performed for 30 min at 30°C and the translation activity of each experiment was measured. Data are shown as the means ± SD from three independent experiments.

Northern blot analysis

To detect *in vitro* transcribed RNA, a luciferase cDNA was used as the probe. The luciferase cDNA was obtained by digesting the pGL3-Basic vector (Promega) with NarI and XbaI. Reaction mixtures (20 μl, as described above) containing 50 ng of *in vitro* transcribed RNA were preincubated or treated after 10 min incubation with 5 pmol of GST–YB-1. After incubation for 30 min in a rabbit reticulocyte lysate system, total RNA was extracted using an RNeasy Miniprep Kit (Qiagen). RNA samples (0.5 μg/lane) were separated on a 1% formaldehyde–agarose gel and transferred onto Biodyne B membranes (Pall, Port Washington, NY). The membrane was

prehybridized and hybridized with [α-^{32}P]dCTP-labeled probe. Radioactivity was analyzed by autoradiograpy.

Transfections and luciferase assays

Cells underwent transient transfection using the LipofectAMINE method. Human lung cancer H1299 cells were plated at a density of 1×10^5 cells/35 mm well the day before transfection. At ~80–90% confluence, the cells were transfected with 1 μg of reporter plasmid DNA or control vector using LipofectAMINE 2000 reagent (Invitrogen). Three hours later, the cells were washed twice with PBS and placed in fresh medium. Twenty-four hours post-transfection, the luciferase activity was measured as described below. The luciferase activity of the transfected cells was measured using the Dual Luciferase Assay System (Promega). Briefly, cells were lysed with 250 μl of 1× Passive Lysis Buffer (Promega). After a brief centrifugation, 10 μl of each supernatant was assayed for luciferase activity. Light emission was measured for 15 s with a luminometer. To standardize translation efficiency, the relative luciferase activity was expressed as the ratio of downstream cistron expression to upstream cistron expression (luciferase/EYFP). The fluorescence of enhanced yellow fluorescent protein (EYFP) was excited at 488 nm and measured for 1 s using a fluorometer.

RESULTS

Analysis of the multiple transcription initiation sites of the YB-1 gene

To investigate the mechanisms of translational control regulating YB-1 protein levels, the possible involvement of YB-1 mRNA was investigated. The 5′-UTR has a high G+C content (61%), suggesting that it could assume a high level of secondary structure *in vivo*. Computer modeling of potential secondary structures suggested that structures with free energies (ΔG values) lower than −190 kcal/mol could be formed (data not shown). We previously identified several transcription initiation sites for the YB-1 gene in KB3-1 and T24 cells (28). To compare the major transcription initiation sites in other cell lines, primer extension analysis was performed (Fig. 1A). The lung cancer cell line H1299 and endothelial cells (HUVECs), were compared with KB3-1 cells. The transcription initiation sites (*) were identical in all of the cells and eight transcripts (*1–*8) were observed in the region mapped to +1 to +197 (Fig. 1B). The ratio of the transcripts differed in each cell line. The proportion of transcripts starting at initiation site *1 was significantly higher in HUVECs, compared to the other cancer cells. These results suggest that the multiple transcription start sites of YB-1 mRNA observed in cell lines may be involved in the regulation of YB-1 protein expression.

The 5′-UTR of YB-1 mRNA increases the expression of a luciferase reporter *in vitro* and *in vivo*

To study the possible involvement of the 5′-UTR of YB-1 mRNA in translation control, we generated two types of reporter constructs. (i) Those containing luciferase cDNA ligated to the full-length 5′-UTR of YB-1 gene (pT7-YB5′-1) and (ii) the non-ligated luciferase control construct (pT7) (Fig. 2A). The predominant 5′ transcription initiation site is

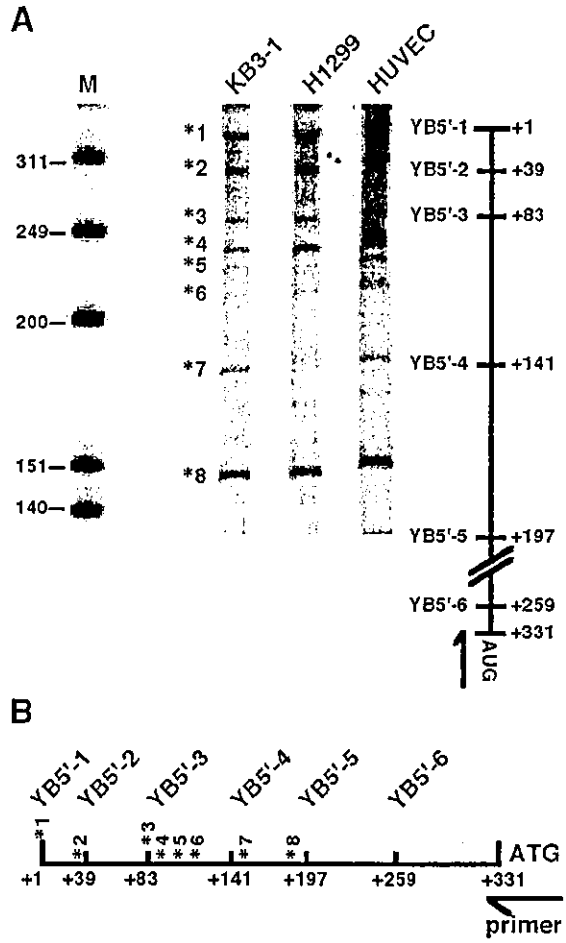

Figure 1. Analysis of the transcription start site of the YB-1 gene by primer extension assay. (A) Primer extension assay. Hybridization of the primer extension was performed with 5′-labeled oligonucleotide and 1 μg poly(A)$^+$ RNA of each cell line. The markers shown on the left are end-labeled HinfI fragments of ϕ-X174 DNA. Black asterisks (*) indicate transcription initiation start sites. The 5′ furthest transcription initiation start site is indicated as +1 and the first AUG codon is indicated at +331. The arrow indicates the position of the primer that was used for extension. The primer hybridizes the sense strand between nucleotides +317 and +337 of the YB-1 gene. (B) Schematic distribution of the transcription initiation site in the YB-1 5′-UTR.

designated +1 in the text and figures. Additional experiments were performed to investigate the regulatory region of the 5′-UTR of YB-1 mRNA. A total of five serial deletion mutants (pT7-YB-5′-2–pT7-YB5′-6) were constructed, each corresponding to a particular transcription initiation site. We first cloned transcripts *1, *2, *4, *7 and *8, which were each expressed at up to 10% of the total. These transcripts corresponded to YB5′-1–YB5′-5. We made an additional probe, YB5′-6, for detection of the shortest 5′-UTR fragment of YB-1. *In vitro* transcription reactions were performed on each of these constructs using T7 RNA polymerase and the integrity of the transcripts was confirmed by gel electrophoresis (data not shown). The differences in the transcript sizes were consistent with the length of the 5′-UTR (Fig. 2A). Equal amounts of the transcripts were translated in rabbit reticulocyte lysate and the luciferase activity was measured. The presence of the full-length 5′-UTR of YB-1 mRNA by itself

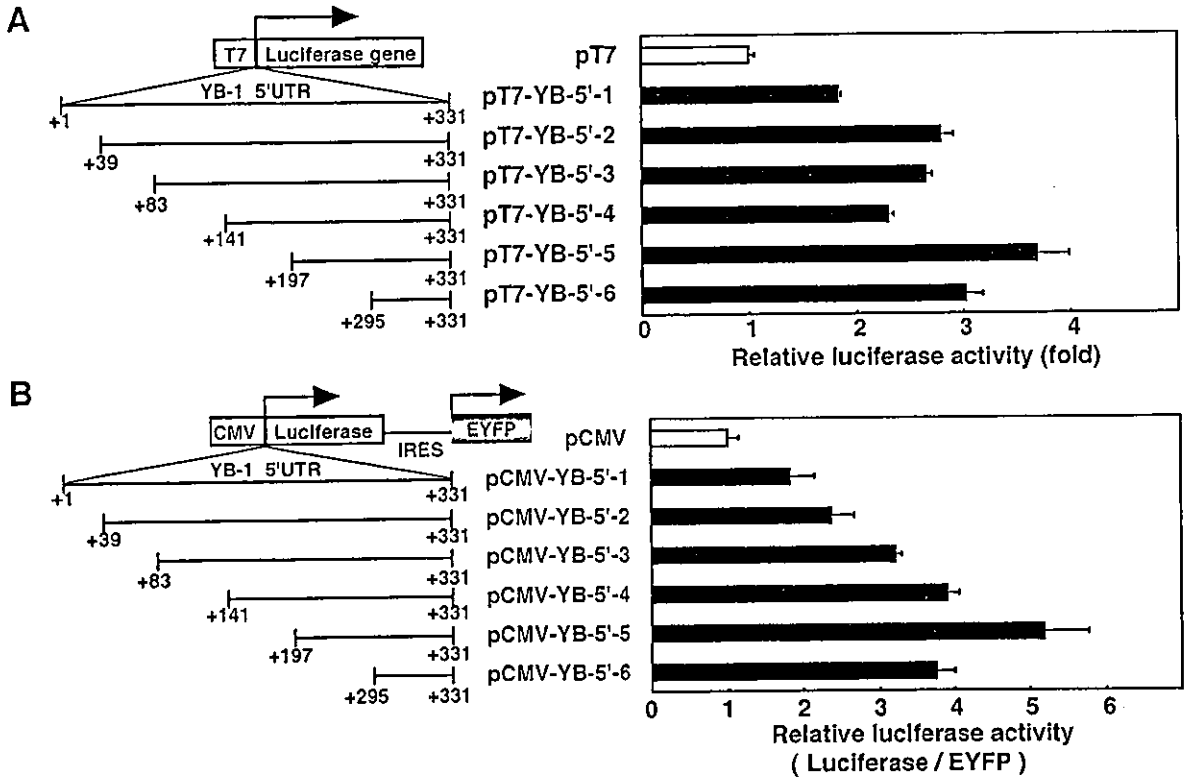

Figure 2. Effect of deletions of the 5′-UTR of YB-1 on the expression of a luciferase reporter *in vitro* and *in vivo*. (**A**) Schematic representation of the reporter constructs containing luciferase cDNA ligated to the YB-1 5′-UTR region (pT7-YB5′-1–pT7-YB5′-6) fragments of various sizes, as well as the non-ligated control construct (pT7). The YB-1 5′-UTR region (pT7-YB5′-1–pT7-YB5′-6) fragments were enlarged to show the limits of regions of the 5′-UTR of YB-1. The right-angled arrow denotes the start site and direction of transcription. Each of the reporter plasmids was transcribed *in vitro* in a reaction driven by T7 RNA polymerase and then 50 ng of the RNA constructs were translated using the rabbit reticulocyte lysate system. The luciferase assay was performed after incubation for 90 min at 30°C. (**B**) Schematic representation of the bicistronic reporter constructs containing luciferase cDNA ligated to the YB-1 5′-UTR region (pCMV-YB5′-1–pCMV-YB5′-6) fragments of various sizes, as well as the non-ligated control construct (pCMV). Each of the reporter plasmids was transcribed under the control of the human cytomegalovirus early promoter (CMV). The right-angled arrow indicates the start site and direction of translation. H1299 cells were transfected with these constructs and their luciferase activities were measured. To standardize the translation efficiency, relative luciferase activity was expressed as the ratio of downstream cistron expression to upstream cistron expression (luciferase/EYFP). Data are shown as the means ± SD (error bars) of three independent experiments.

increased the level of luciferase activity ~2-fold relative to that of the control mRNA (pT7). Furthermore, each of the YB-1 5′-UTR deletion constructs showed higher translational activity than did the pT7 control. Of all the constructs, pT7-YB5′-5 showed the highest activity, which was ~4-fold greater than that of the control construct (Fig. 2A).

We next determined whether a similar increase in activity could also be induced in cultured cells by the 5′-UTR. We constructed eukaryotic expression vectors containing luciferase cDNA ligated to various regions of the YB-1 5′-UTR (pCMV-YB5′-1–pCMV-YB5′-6), as described for the *in vitro* experiment (Fig. 2A). The reporter constructs were transcribed under control of the human cytomegalovirus early promoter. After transfection into a H1299 lung carcinoma cell line, the levels of luciferase activity were compared (Fig. 2B). As observed with the *in vitro* translation assays (Fig. 2A), the YB-1 5′-UTR increased the level of luciferase expression. The full-length YB-1 5′-UTR by itself increased luciferase activity ~2-fold compared to the control construct (pCMV). Furthermore, pCMV-YB5′-5 also showed the highest activity, which was 4–5-fold that of the control. The mRNAs encoded by the reporter constructs were equally expressed, as determined by northern blot analysis (data not shown). These results suggest that the YB-1 5′-UTR enables more efficient translation of mRNA *in vitro* and *in vivo* and the short-length construct (YB5′-5) facilitates the most efficient translational activity.

YB-1 binds its own mRNA in the cytoplasm

YB-1, which posseses RNA binding activity (26), has been reported to be involved in translational regulation and in the regulation of mRNA stability (16). In order to identify whether or not YB-1 protein interacts with its own mRNA in the cytoplasm, we performed RT–PCR using mRNA isolated by co-immunoprecipitation with YB-1 immunoprecipitant (Fig. 3). Flag–YB-1 or an empty Flag expression vector were transfected into an H1299 lung carcinoma cell line. After 48 h, cells were lysed and YB-1 proteins were immunoprecipitated with Flag antibody. The mRNA was purified after immunoprecipitation and amplified by RT–PCR using YB-1- and β-actin-specific primers. YB-1 mRNA and β-actin mRNA were both expressed in the H1299 cell lines (Fig. 3, lane 4).

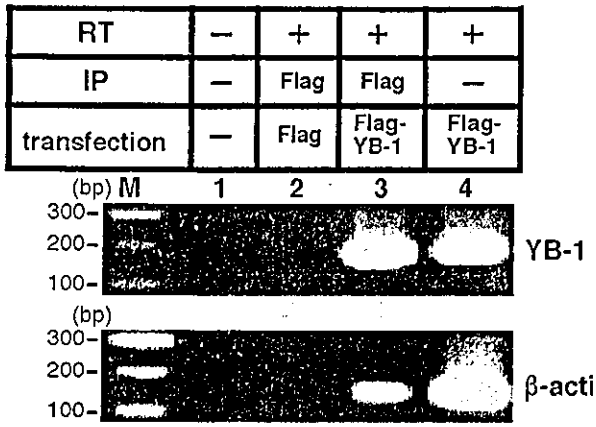

Figure 3. YB-1 interacts with its own mRNA in the cytoplasm. Flag–YB-1 or Flag expression vector was transfected into H1299 cells. After 48 h, cells were lysed and the YB-1 proteins were immunoprecipitated (IP) with Flag antibody. The mRNA were purified after immunoprecipitation and amplified by RT–PCR with YB-1- (upper panel) and β-actin-specific (lower panel) primers. The RT–PCR amplification products were analyzed by 2% agarose gel electrophoresis.

Flag–YB-1 immunoprecipitates contained YB-1 mRNA (Fig. 3, lane 3), while the control Flag immnoprecipitate did not (Fig. 3, lane 2). Furthermore, the YB-1 immunoprecipitate also contained β-actin mRNA (Fig. 3, lane 3). These data provide evidence that YB-1 interacts with its own mRNA and β-actin mRNA in the cytoplasm of cultured cells.

YB-1 binds to the 5′-UTR of its cognate mRNA through a C-terminal domain

We next investigated the interaction of YB-1 protein with the 5′-UTR of its own mRNA *in vitro*. An RNA gel shift assay (REMSA) was performed by using KB3-1 and H1299 cell lysates and an *in vitro* synthesized mRNA probe corresponding to the full-length 5′-UTR of YB-1 mRNA (Fig. 4A). YB-1 5′-UTR formed an RNA–protein complex with lysates made using KB3-1 and H1299 cell lysates (Fig. 4A, lanes 2–4 and 8–10). The presence of endogenous YB-1 protein in the major complex was confirmed by the ability of a YB-1-specific antibody to supershift most of the complex (Fig. 4A, lanes 6 and 12). To determine whether YB-1 protein is able to directly interact with the 5′-UTR of YB-1 mRNA, we performed a REMSA using purified recombinant YB-1 (Fig. 4B). Recombinant YB-1 also clearly bound to the 5′-UTR of YB-1 mRNA (Fig. 4B, lanes 5–7), while control GST protein did not (Fig. 4B, lanes 2–4). The interaction with YB-1 protein was also confirmed by the use of YB-1-specific antibody (Fig. 4B, lanes 10 and 11).

We previously observed that rabbit p50, a homolog of human YB-1 protein, was present in rabbit reticulocyte lysate. To assess the nature of the rabbit p50 interaction with the 5′-UTR of YB-1 mRNA, we performed a REMSA using rabbit reticulocyte lysate (Fig. 4C). When added to rabbit reticulocyte lysate, the YB-1 5′-UTR formed an RNA–protein complex (Fig. 4C, lanes 2 and 3). The presence of rabbit p50 in the major complex was confirmed by the ability of a YB-1-specific antibody to supershift most of the complex (Fig. 4C, lane 5).

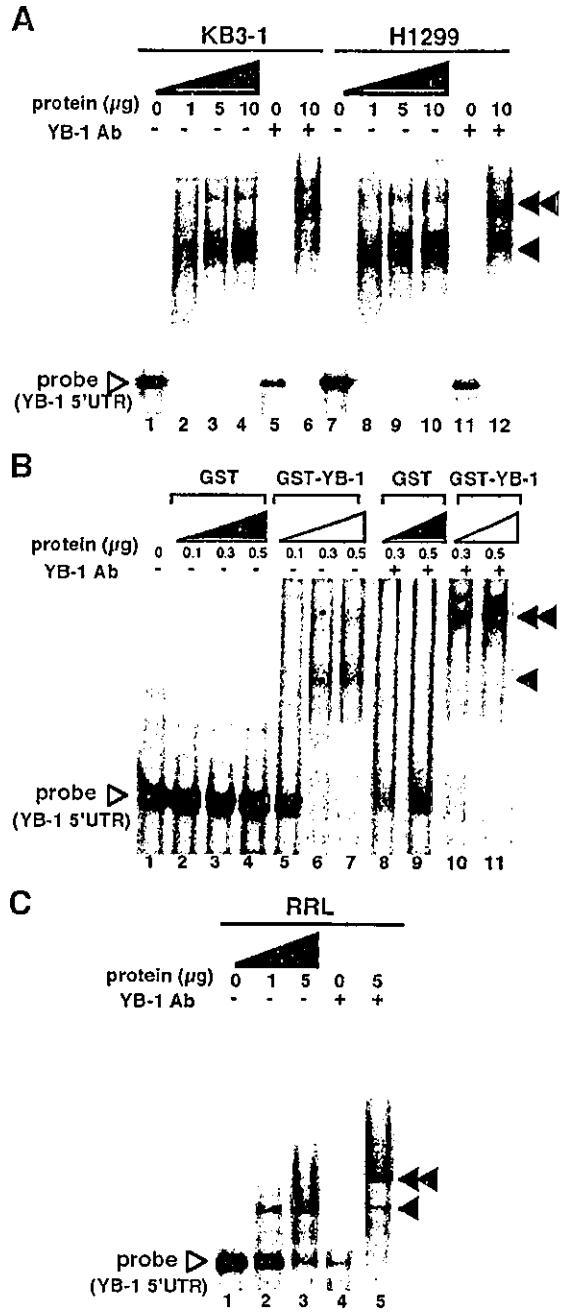

Figure 4. YB-1 binds to the 5′-UTR region of YB-1 mRNA. (A) Endogenous YB-1 protein binds to the 5′-UTR region of YB-1 mRNA in the cytoplasm. The indicated amounts of KB3-1 and H1299 cell lysate were incubated with ^{32}P-labeled YB-1 5′-UTR RNA at 25°C for 15 min. An aliquot of 2 μg YB-1-specific antibody (Ab) was added to lanes 5, 6, 11 and 12. An arrow indicates the YB-1/YB-1 5′-UTR RNA complex and a double-headed arrow indicates supershifted complexes. (B) Purified YB-1 binds to YB-1 5′-UTR RNA. The indicated amount of GST or GST–YB-1 fusion was incubated with ^{32}P-labeled YB-1 5′-UTR RNA at 25°C for 15 min. An aliquot of 2 μg YB-1-specific antibody (Ab) was added to lanes 8–11. An arrow indicates the YB-1/YB-1 5′-UTR RNA complex and a double-headed arrow indicates supershifted complexes. (C) Rabbit YB-1 (p50) binds to the 5′-UTR region of YB-1 mRNA in the *in vitro* translation system. The indicated amounts of rabbit reticulocyte lysate (RRL) were incubated with ^{32}P-labeled YB-1 5′-UTR RNA at 25°C for 15 min. An aliquot of 2 μg YB-1-specific antibody (Ab) was added to lanes 4 and 5. An arrow indicates the rabbit YB-1/YB-1 5′-UTR RNA complex and a double-headed arrow indicates supershifted complexes. YB-1/YB-1 5′-UTR RNA probe complexes were separated as described above.

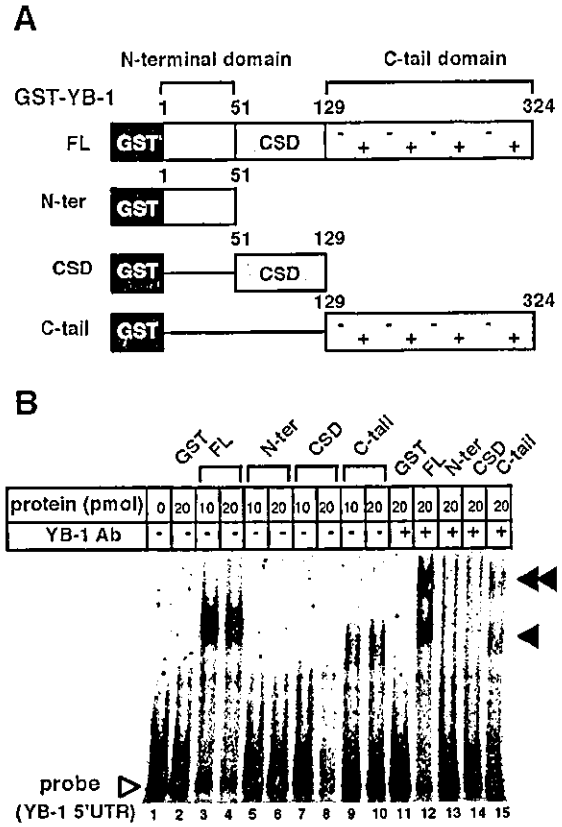

Figure 5. Identification of the YB-1 5′-UTR binding domain in YB-1. A) Schematic illustration of the GST–YB-1 deletion mutants used in this study. CSD indicates the cold shock domain. (B) REMSA assay. The indicated amount of each GST–YB-1 deletion mutant and GST was incubated with ^{32}P-labeled YB-1 5′-UTR RNA at 25°C for 15 min. An aliquot of 2 μg YB-1-specific antibody (Ab) was added to lanes 11–15. An arrow indicates the YB-1/YB-1 5′-UTR RNA complex and a double-headed arrow indicates supershifted complexes. YB-1 mutant/YB-1 5′-UTR RNA probe complexes were separated using 4% native polyacrylamide gels.

YB-1 protein consists of three major domains, each of which has the potential to bind nucleic acids (30): the alanine/proline-rich N-terminal domain, the highly conserved nucleic acid binding domain and the C-tail domain. To identify which domains of YB-1 protein are responsible for this interaction, we performed a REMSA using a series of GST fusion proteins containing either full-length YB-1 (FL) or the mutant derivatives GST–YB-1 N-ter, CSD and C-tail (Fig. 5A). A strong interaction was observed using the full-length YB-1 (Fig. 5B, lanes 3 and 4) and the C-tail of YB-1 (Fig. 5B, lanes 9 and 10). The central CSD, containing the RNP1 motif, was not able to bind to the 5′-UTR of YB-1 mRNA (Fig. 5B, lanes 7 and 8). The binding activity of both constructs resulted in the appearance of a supershifted band in the presence of a YB-1-specific antibody that recognizes the C-terminal tail of YB-1 (Fig. 5B, lanes 12 and 15). These results suggest that the C-tail domain of YB-1 protein interacts with the 5′-UTR of its own mRNA, independent of other domains.

Identification of the YB-1 binding region in the 5′-UTR of YB-1 mRNA

To identify which region of the YB-1 mRNA 5′-UTR interacts with YB-1 protein, we performed a REMSA using probes

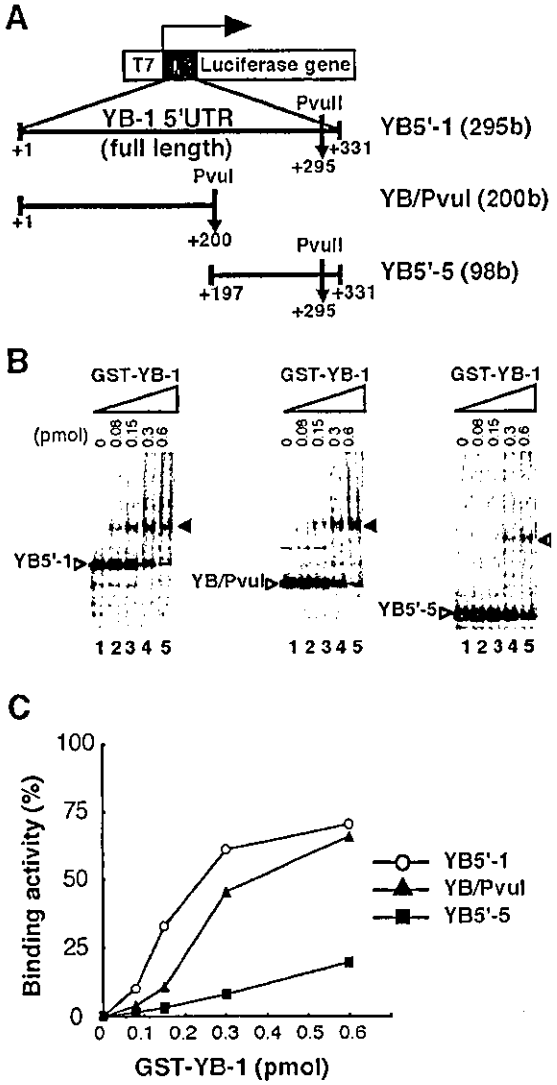

Figure 6. Identification of the YB-1 binding region in YB-1 5′-UTR mRNA. (A) Schematic illustration of YB-1 5′-UTR deletion constructs used as the probe in a REMSA. To produce RNA of defined length, restriction enzyme (PvuI or PvuII) was used to linearize the DNA templates. (B) REMSA. The indicated amount of GST–YB-1 fusion was incubated with each ^{32}P-labeled YB-1 5′-UTR deletion mRNA at 25°C for 15 min. An arrow indicates the YB-1/YB-1 5′-UTR RNA complex. YB-1/YB-1 5′-UTR RNA probe complexes were separated using 4% native polyacrylamide gels. (C) Kinetic analysis of GST–YB-1 binding to YB5′-1, YB/PvuI and YB5′-5 probes. The GST–YB-1 binding activity to YB-1 5′-UTR fragments identical to that shown in (B) were quantified by monitoring amounts of the binding complexes.

corresponding to YB5′-1 (295 bases), YB/PvuI (200 bases) and YB5′-5 (98 bases), as defined in Figure 1B (Fig. 6A). All three constructs formed RNA–protein complexes in a dose-dependent manner. However, the affinity of YB-1 for the three probes differed. When GST–YB-1 was added to the full-length YB-1 5′-UTR (YB5′-1) and YB/PvuI, a retarded complex was clearly visible (Fig. 6B). When 0.6 pmol of GST–YB-1 was added, up to 60% of the YB5′-1 and YB/PvuI probes were bound to GST–YB-1 (Fig. 6C). However, little retarded band was observed using the deleted YB5′-5 probe (Fig. 6B) when the same amount of YB-1 was used. When 0.6 pmol of YB-1 was added to YB5′-5, <20% YB5′-5 was

bound. These results indicate that YB-1 protein binds to the full-length and the first half of the YB-1 5′-UTR more efficiently than a construct containing the second half of the YB-1 5′-UTR, YB5′-5.

Recombinant YB-1 protein decreases translation through its own 5′-UTR mRNA element *in vitro*

As shown in the REMSA, we observed higher affinity binding to the full-length 5′-UTR of YB-1 mRNA with recombinant YB-1. It has been shown that inhibitory concentrations of YB-1 suppressed the interaction with initiation complexes such as eIF4E, eIF4A and eIF4B, and these concentrations inhibited translation at the stage of initiation (17,31). YB-1 has also been reported to affect the translation of both cap$^+$ poly(A)$^+$ and cap$^-$ poly(A)$^-$ mRNAs (1,2). Skabkina *et al.* also demonstrated that poly(A) binding protein positively affects YB-1 mRNA translation through specific interaction with YB-1 mRNA (32). Thus, we investigated whether or not recombinant YB-1 inhibits translation in a cell-free translation system by using the full-length and deleted YB-1 5′-UTR constructs. In this system the transcript of YB-1 5′-UTR were neither capped nor polyadenylated. We therefore excluded the possibility that binding between YB-1 protein and translation initiation and elongation factors such as cap binding protein or poly(A) binding protein was involved. To test the functional activity of YB-1 protein, recombinant YB-1 protein was added to the *in vitro* translation system. *In vitro* transcripts from pT7, pT7-YB5′-1 and pT7-YB5′-5 were translated in a rabbit reticulocyte lysate system in the absence or presence of recombinant YB-1 protein and the luciferase activity was measured. As shown in Figure 7A, the addition of YB-1 at the start of translation inhibited the translation of all three constructs in a dose-dependent manner to a maximum of ~60%.

Next, we measured the kinetics of luciferase translation in a rabbit retilculocyte lysate. After the first 10 min, almost 10% of translation had occurred and translation efficiency was saturated after 60 min (data not shown). To investigate the inhibitory effects of YB-1 protein on translation, we added various amounts of YB-1 protein 10 min after translation was started (Fig. 7B). The addition of YB-1 10 min after translation inhibited the luciferase activity in a dose-dependent manner when the construct containing the full-length 5′-UTR (pT7-YB5′-1) was used; this reduction amounted to ~50% with 5 pmol of YB-1, implying that only 10% of the inhibition results from translation that could have occurred in the first 10 min of the 30 min reaction. On the other hand, little YB-1-dependent repression of translation was seen using pT7-YB5′-5 and pT7-luciferase. These results suggested that pretreated YB-1 inhibited translation of all constructs and the addition of YB-1 after translation also specifically inhibited translation of the construct with the full-length 5′-UTR.

YB-1 protein was also involved in stabilization of mRNA in rabbit reticulocyte system. We confirmed the integrity of the *in vitro* transcribed mRNA by northern blot analysis before and after treatment with YB-1 (Fig. 7C). No change in transcribed RNA stability was observed with up to 30 min incubation in rabbit reticulocyte system (Fig. 7C, lanes 1–3, 4–6 and 7–9).

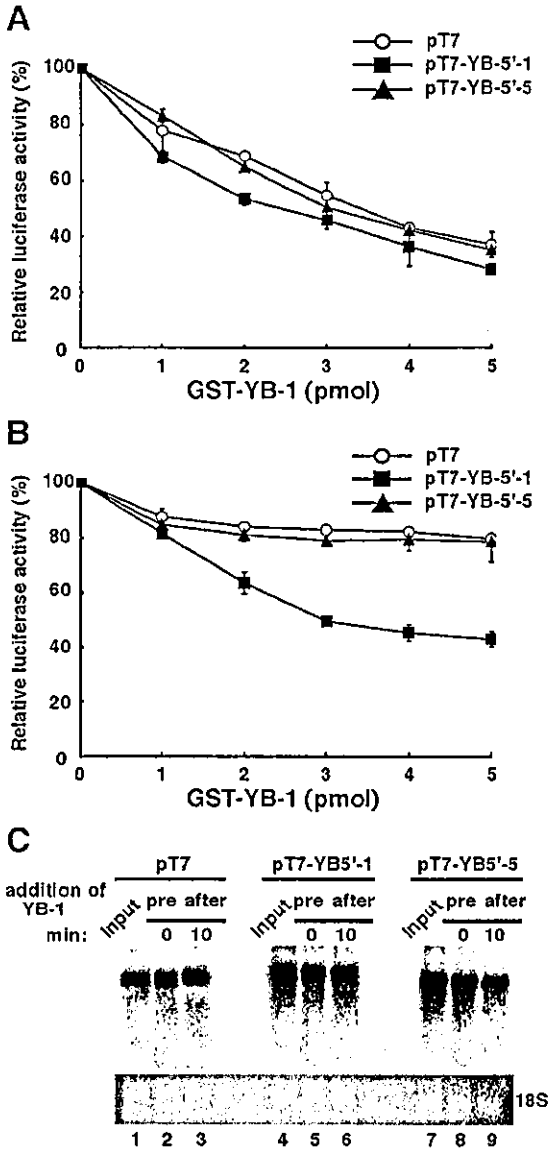

Figure 7. Characterization of translation inhibition by YB-1 protein through its own 5′-UTR mRNA element *in vitro*. The indicated amounts of GST–YB-1 fusion were added to a rabbit reticulocyte lysate system either initially (A) or after 10 min incubation (B) using 50 ng of the RNA constructs described in Figure 2A. The *in vitro* translation was performed for 30 min at 30°C and the translational products were directly used for the luciferase assay. Data are shown as means ± SD (error bars) of three independent experiments. (C) The effect of YB-1 on mRNA stability was examined. An aliquot of 50 ng of *in vitro* transcribed RNA constructs was preincubated (pre) or treated after 10 min incubation (after) with 5 pmol of GST–YB-1. After incubation for 30 min in a rabbit reticulocyte lysate system, the RNA was detected by northern blot hybridization. Lanes 1, 4 and 7 (Input) show the *in vitro* transcribed RNA constructs isolated from the exact at 0 min incubation.

Recombinant YB-1 protein did not decrease translation through a mutant 5′-UTR element

Next, we focused on the possible secondary structure of the full-length 5′-UTR of YB-1 mRNA. In general, the stem–loop structure found in 5′-UTRs of mRNAs affect their translational efficiency as, for example, in the ferritin 5′-UTR (18). In

the YB-1 5′-UTR, we observed three regions which are predicted to form possible stem–loop structures. To investigate the translational regulatory region of the 5′-UTR of YB-1 mRNA, we constructed three mutants which disrupt the stem–loop structure. These contained internal mutations (mut1–mut3) which we have designated using the nucleotide at the 5′ end corresponding to the transcription initiation site (*) (Fig. 8A). To characterize the translational inhibition observed with the addition of YB-1, we performed cell-free translational assays using mutants of the above constructs of the YB-1 5′-UTR fused to luciferase mRNA (Fig. 8B and C). The addition of YB-1 at the start of translation resulted in up to a 60% inhibition of luciferase activity in a dose-dependent manner, in the case of both the mutant and full-length 5′-UTR (Fig. 8B). However, no repression of the luciferase activity of these mutant constructs (pT7-YBM1–pT7-YBM3) was observed when YB-1 was added 10 min after translation was initiated (Fig. 8C). These results suggest that YB-1 protein regulates the translation of all constructs and also that it specifically inhibits translation when the 5′-UTR of YB-1 mRNA is present. Our findings are consistent with a model in which YB-1 protein specifically binds to the full-length 5′-UTR of YB-1 mRNA and inhibits its own translation *in vitro*.

DISCUSSION

In this report, our data demonstrate that YB-1 protein not only binds to an RNA containing the human YB-1 5′-UTR *in vitro* and *in vivo*, but that it also exhibits functional activity by specifically inhibiting the translation of a YB-1 5′-UTR–luciferase reporter mRNA in rabbit reticulocyte lysate assays. The multifunctional protein YB-1 was first identified as a transcription factor which binds to the Y-box of the MHC class II promoter sequence (33). Recent studies have demonstrated that YB-1 regulates gene expression not only at the level of transcription, but also at the level of mRNA translation. Considering these characteristics, it is possible that YB-1 might regulate its own expression at the translational level.

The present paper provides evidence that the translational control of YB-1 expression is mediated via the 5′-UTR of YB-1 mRNA. Global control of translational efficiency can be achieved by regulating the phosphorylation state of an array of initiation factors (such as eIF2 and eIF4E). However, control of translational initiation on an individual mRNA is determined primarily by its nucleotide sequence and the secondary structure of the regulatory protein. The 5′-UTR plays a particularly important role in the regulation of translation initiation via an interaction with RNA binding proteins or by secondary structure formation, which hinders the activity of the translational machinery. Analysis of the 5′-UTR sequence of YB-1 (331 bases in length) revealed several important features that are known to influence translation.

Many *in vitro* and *in vivo* studies have shown that mRNAs with a high likelihood of forming a stable secondary structure in the 5′-UTR tend to be inefficiently translated (34). However, in both *in vitro* and *in vivo* experiments we found that the 5′-UTR sequence of YB-1 mRNA, with its high G+C content, acts as a potent translational enhancer. The full-length 5′-UTR of YB-1 mRNA increased the level of translation activity and cloning a 134 base region of the YB-1 5′-UTR

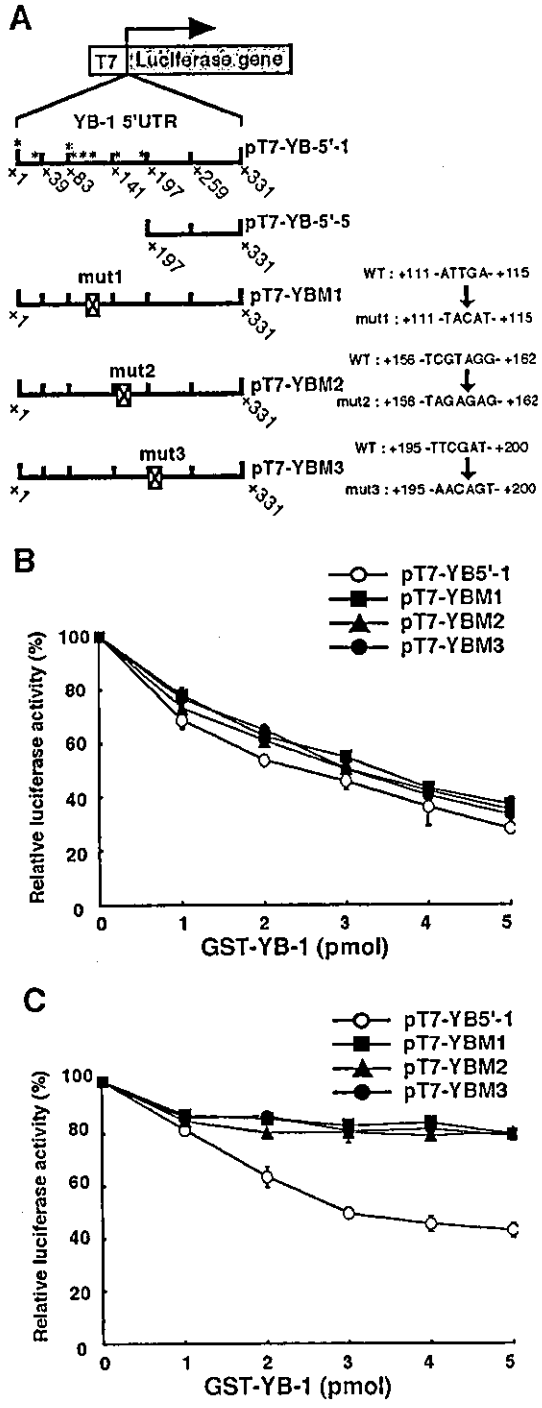

Figure 8. Effect of mutation of the YB-1 5′-UTR mRNA element on translation. (A) Schematic representation of the YB-1 5′-UTR–luciferase fusion reporter constructs used in this study. pT7-YBM1–3 containing an internal mutation (mut1-3), designated by the nucleotide at the 5′ end that corresponded to the transcription initiation sites (*) (see Fig. 1A). (B and C) The characterization of translation inhibition by each reporter construct was compared to that of the other constructs. The indicated amounts of GST–YB-1 fusion were added to a rabbit reticulocyte lysate system either initially (B) or after 10 min incubation (C) using 50 ng of the RNA constructs described in (A). The *in vitro* translation was performed for 30 min at 30°C and the translation activity of each experiment was measured. Data are shown as the means ± SD (error bars) of three independent experiments.

upstream of the coding initiation sequence was also associated with a significant increase in translation activity (Fig. 2A and B). This region might therefore be crucial for the translation activity of the 5′-UTR of YB-1 mRNA. These data suggest that elements within the 5′-UTR of YB-1 mRNA can act as enhancers of mRNA translation.

According to the scanning mechanism postulated for translation initiation, the small (40S) ribosomal subunit enters at the 5′ end of the mRNA and migrates linearly, stopping when the first AUG codon is reached (35). Nekrasov *et al.* (31) demonstrated that YB-1 protein inhibited the initiation step of translation, but did not inhibit the elongation step. Rabbit YB-1 displays both RNA melting and annealing activities in a dose-dependent manner; a relatively low amount of YB-1 promotes the formation of RNA duplexes, whereas an excess of YB-1 causes unwinding of double-stranded forms (36). It is also possible that YB-1 additionally facilitates movement of the small ribosomal subunit to the initiation codon complexed with initiator $tRNA^{Met}$. This may occur up to the initiation codon by YB-1 melting the secondary structure in the mRNA 5′-UTR (31).

In this study, we observed that YB-1 inhibited the translation of all of the transcripts of YB-1 5′-UTR that lacked sequence specificity, suggesting that YB-1 reduced the translation efficiency of 5′-UTR elements, either at the initiation step or by binding directly to the whole RNA. These results provided evidence that YB-1 might block the first step in mRNA recruitment into translation initiation.

The addition of YB-1 10 min after initiation inhibited translational activity only when the full-length 5′-UTR of YB-1 mRNA was present (Figs 7B and 8C). No repression of the luciferase activity of the deleted or mutant constructs (pT7-YBM1–pT7-YBM3) (with disrupted stem–loop structures) was observed. We also observed that YB-1 binds to the first half-region of YB-1 5′ UTR RNA more efficiently than does the latter half construct comprising the second half (Fig. 7). The affinity of YB-1 for the mutated probes was the same as for the wild-type YB5′-1 probes (data not shown). These results suggest that ribosome scanning or ongoing translation might be required for repression by YB-1 when the full-length YB-1 5′-UTR was used. And when mutated and deleted probe were used, YB-1 did not affect ribosomal scanning due to alterations in the secondary structure of the YB-1 5′ UTR. The precise secondary structures of the YB-1 5′-UTR remains to be determined.

By combining the results presented here with previous data, we are able to describe the effect of YB-1 on translation. First, YB-1 blocks the initial step in mRNA recruitment to translation initiation, YB-1 then turns off the interaction of the mRNA with eIF4F (31). Second, YB-1 promotes movement of the small ribosomal subunit within the complex by melting the mRNA 5′-UTR secondary structure, suggesting that YB-1 affects ribosome scanning through the 5′-UTR.

The 5′-UTR plays an important role in regulation of the expression of a number of genes. For instance, the UTRs of mRNAs encoding heat shock proteins (HSPs), known to protect cells against a wide variety of stresses, including heat shock, viral infection and exposure to oxidative free radicals and toxic metal ions (37), have been reported to contain elements important for the post-transcriptional regulation of these key components of the stress response (38,39).

YB-1 has been reported to be involved in the regulation of stress-inducible target genes (40,41), suggesting that YB-1 itself is a stress-activated protein. YB-1 mRNA accumulates in cells when they are treated with UV irradiation or anticancer agents. We previously reported that c-myc and p73 activate YB-1 transcription and may regulate important biological processes via their effects on YB-1 gene expression (42). Additional experiments are needed to confirm the role of YB-1 in regulating translation *in vivo* under various stress conditions. It would be of interest to determine how the 5′-UTR of YB-1 mRNA affects the translation of YB-1 in response to extracellular stimuli or environmental stress.

The translational control of gene expression has been identified as an important regulatory mechanism for many gene products involved in the regulation of proliferation [e.g. c-mos (43), FGF-2 (44,45), PDGF-B (46), p27 (47) and cdk4 (48)]. The tumor suppressor p53 has been implicated in the translational regulation of both p53 and cdk4 mRNAs (49). Similarly, several distinct components of the translation apparatus have been shown to be deregulated or overexpressed in human tumors. So, it is of note that the level of the YB-1 mRNA from the 5′ furthest transcription initiation start site was significantly higher in HUVEC cells, compared to the other cancer cell lines examined (Fig. 1). The deregulation of the translational control of YB-1 might therefore also play a role in tumor progression.

In conclusion, YB-1 protein binds to an RNA containing the 5′-UTR of human YB-1 mRNA *in vitro* and *in vivo* and exhibits functional activity by inhibiting the translation of a YB-1 5′-UTR–luciferase reporter mRNA through the aid of its own 5′-UTR mRNA. We propose a model in which YB-1 protein autoregulates its own translation by binding to the 5′-UTR of its own mRNA. Our results support a *trans*-acting repressor hypothesis, in which a repressor protein specifically binds to its own 5′-UTR element, resulting in translational repression and the maintenance of constant protein levels.

ACKNOWLEDGEMENTS

We would like to thank Prof. R.G. Deeley for helpful discussions and for critically reading this manuscript. This work was supported by the Second-Term Comprehensive Ten-Year Strategy for Cancer Control from the Ministry of Health and Welfare of Japan and by the Cancer Research Fund from the Ministry of Education, Culture, Sports, Science and Technology.

REFERENCES

1. Pisarev,A.V., Skabkin,M.A., Thomas,A.A., Merrick,W.C., Ovchinnikov,L.P. and Shatsky,I.N. (2002) Positive and negative effects of the major mammalian messenger ribonucleoprotein p50 on binding of 40 S ribosomal subunits to the initiation codon of beta-globin mRNA. *J. Biol. Chem.*, **277**, 15445–15451.
2. Evdokimova,V.M., Kovrigina,E.A., Nashchekin,D.V., Davydova,E.K., Hershey,J.W. and Ovchinnikov,L.P. (1998) The major core protein of messenger ribonucleoprotein particles (p50) promotes initiation of protein biosynthesis *in vitro*. *J. Biol. Chem.*, **273**, 3574–3581.
3. Davydova,E.K., Evdokimova,V.M., Ovchinnikov,L.P. and Hershey,J.W. (1997) Overexpression in COS cells of p50, the major core protein associated with mRNA, results in translation inhibition. *Nucleic Acids Res.*, **25**, 2911–2916.

4. Kohno,K., Izumi,H., Uchiumi,T. and Kuwano,M. (2003) The pleiotropic functions of the Y-box-binding protein, YB-1. *Bioessays*, **25**, 691–698.
5. Wolffe,A.P. (1994) Structural and functional properties of the evolutionarily ancient Y-box family of nucleic acid binding proteins. *Bioessays*, **16**, 245–251.
6. Ladomery,M. and Sommerville,J. (1995) A role for Y-box proteins in cell proliferation. *Bioessays*, **17**, 9–11.
7. Swamynathan,S.K., Nambiar,A. and Guntaka,R.V. (1998) Role of single-stranded DNA regions and Y-box proteins in transcriptional regulation of viral and cellular genes. *FASEB J.*, **12**, 515–522.
8. Matsumoto,K. and Wolffe,A.P. (1998) Gene regulation by Y-box proteins: coupling control of transcription and translation. *Trends Cell Biol.*, **8**, 318–323.
9. Sommerville,J. (1999) Activities of cold-shock domain proteins in translation control. *Bioessays*, **21**, 319–325.
10. Swamynathan,S.K., Nambiar,A. and Guntaka,R.V. (2000) Chicken Y-box proteins chk-YB-1b and chk-YB-2 repress translation by sequence-specific interaction with single-stranded RNA. *Biochem. J.*, **348**, 297–305.
11. Kelm,R.J.,Jr, Cogan,J.G., Elder,P.K., Strauch,A.R. and Getz,M.J. (1999) Molecular interactions between single-stranded DNA-binding proteins associated with an essential MCAT element in the mouse smooth muscle alpha-actin promoter. *J. Biol. Chem.*, **274**, 14238–14245.
12. Kelm,R.J.,Jr, Elder,P.K. and Getz,M.J. (1999) The single-stranded DNA-binding proteins, Puralpha, Purbeta and MSY1 specifically interact with an exon 3-derived mouse vascular smooth muscle alpha-actin messenger RNA sequence. *J. Biol. Chem.*, **274**, 38268–38275.
13. Gu,W., Tekur,S., Reinbold,R., Eppig,J.J., Choi,Y.C., Zheng,J.Z., Murray,M.T. and Hecht,N.B. (1998) Mammalian male and female germ cells express a germ cell-specific Y-Box protein, MSY2. *Biol. Reprod.*, **59**, 1266–1274.
14. Herbert,T.P. and Hecht,N.B. (1999) The mouse Y-box protein, MSY2, is associated with a kinase on non-polysomal mouse testicular mRNAs. *Nucleic Acids Res.*, **27**, 1747–1753.
15. Matsumoto,K., Meric,F. and Wolffe,A.P. (1996) Translational repression dependent on the interaction of the *Xenopus* Y-box protein FRGY2 with mRNA. Role of the cold shock domain, tail domain and selective RNA sequence recognition. *J. Biol. Chem.*, **271**, 22706–22712.
16. Chen,C.Y., Gherzi,R., Andersen,J.S., Gaietta,G., Jurchott,K., Royer,H.D., Mann,M. and Karin,M. (2000) Nucleolin and YB-1 are required for JNK-mediated interleukin-2 mRNA stabilization during T-cell activation. *Genes Dev.*, **14**, 1236–1248.
17. Evdokimova,V., Ruzanov,P., Imataka,H., Raught,B., Svitkin,Y., Ovchinnikov,L.P. and Sonenberg,N. (2001) The major mRNA-associated protein YB-1 is a potent 5′ cap-dependent mRNA stabilizer. *EMBO J.*, **20**, 5491–5502.
18. Ashizuka,M., Fukuda,T., Nakamura,T., Shirasuna,K., Iwai,K., Izumi,H., Kohno,K., Kuwano,M. and Uchiumi,T. (2002) Novel translational control through an iron-responsive element by interaction of multifunctional protein YB-1 and IRP2. *Mol. Cell. Biol.*, **22**, 6375–6383.
19. Wilkie,G.S., Dickson,K.S. and Gray,N.S. (2003) Regulation of mRNA translation by 5′- and 3′-UTR-binding factors. *Trends Biochem. Sci.*, **4**, 182–188.
20. Pesole,G., Liuni,S., Grillo,G., Licciulli,F., Mignone,F., Gissi,C. and Saccone,G. (2002) UTRdb and UTRsite: specialized databases of sequences and functional elements of 5′ and 3′ untranslated region of eukaryotic mRNAs. Update 2002. *Nucleic Acids Res.*, **1**, 335–340.
21. McCarthy,J.E. and Kollmus,H. (1995) Cytoplasmic mRNA-protein interactions in eukaryotic gene expression. *Trends Biochem. Sci.*, **20**, 191–197.
22. Macdonald,P. (2001) Diversity in translational regulation. *Curr. Opin. Cell Biol.*, **13**, 326–331.
23. Sonenberg,N. (1994) mRNA translation: influence of the 5′ and 3′ untranslated regions. *Curr. Opin. Genet. Dev.*, **4**, 310–315.
24. Ise,T., Nagatani,G., Imamura,T., Kato,K., Takano,H., Nomoto,M., Izumi,H., Ohmori,H., Okamoto,T., Ohga,T., Uchiumi,T., Kuwano,M. and Kohno,K. (1999) Transcription factor Y-box binding protein 1 binds preferentially to cisplatin-modified DNA and interacts with proliferating cell nuclear antigen. *Cancer Res.*, **59**, 342–346.
25. Okamoto,T., Izumi,H., Imamura,T., Takano,H., Ise,T., Uchiumi,T., Kuwano,M. and Kohno,K. (2000) Direct interaction of p53 with the Y_-box binding protein, YB-1: a mechanism for regulation of human gene expression. *Oncogene*, **19**, 6194–6202.
26. Izumi,H., Imamura,T., Nagatani,G., Ise,T., Murakami,T., Uramoto,H., Torigoe,T., Ishiguchi,H., Yoshida,Y., Nomoto,M., Okamoto,T., Uchiumi,T., Kuwano,M., Funa,K. and Kohno,K. (2001) Y box-binding protein-1 binds preferentially to single-stranded nucleic acids and exhibits 3′→5′ exonuclease activity. *Nucleic Acids Res.*, **29**, 1200–1207.
27. Ohga,T., Koike,K., Ono,M., Makino,Y., Itagaki,Y., Tanimoto,M., Kuwano,M. and Kohno,K. (1996) Role of the human Y box-binding protein YB-1 in cellular sensitivity to the DNA-damaging agents cisplatin, mitomycin C and ultraviolet light. *Cancer Res.*, **56**, 4224–4228.
28. Makino,Y., Ohga,T., Toh,S., Koike,K., Okumura,K., Wada,M., Kuwano,M. and Kohno,K. (1996) Structural and functional analysis of the human Y-box binding protein (YB-1) gene promoter. *Nucleic Acids Res.*, **24**, 1873–1878.
29. Mullner,E.W., Neupert,B. and Kuhn,L.C. (1989) A specific mRNA binding factor regulates the iron-dependent stability of cytoplasmic transferrin receptor mRNA. *Cell*, **58**, 373–382.
30. Ladomery,M. and Sommerville,J. (1994) Binding of Y-box proteins to RNA: involvement of different protein domains. *Nucleic Acids Res.*, **22**, 5582–5589.
31. Nekrasov,M.P., Ivshina,M.P., Chernov,K.G., Kovrigina,E.A., Evdokimova,V.M., Thomas,A.A., Hershey,J.W. and Ovchinnikov,L.P. (2003) The mRNA-binding protein YB-1 (p50) prevents association of the initiation factor eIF4G with mRNA and inhibits protein synthesis at the initiation stage. *J. Biol. Chem.*, **278**, 13936–13943.
32. Skabkina,O.V., Skabkin,M.A., Popova,N.V., Lyabin,D.N., Penalva,L.O. and Ovchinnikov,L.P. (2003) Poly(A)-binding protein positively affects YB-1 mRNA translation through specific interaction with YB-1 mRNA. *J. Biol. Chem.*, **278**, 18191–18198.
33. Didier,D.K., Schiffenbauer,J., Woulfe,S.L., Zacheis,M. and Schwartz,B.D. (1988) Characterization of the cDNA encoding a protein binding to the major histocompatibility complex class II Y box. *Proc. Natl Acad. Sci. USA*, **85**, 7322–7326.
34. Kozak,M. (1991) Structural features in eukaryotic mRNAs that modulate the initiation of translation. *J. Biol. Chem.*, **266**, 19867–19870.
35. Kozak,M. (2002) Pushing the limits of the scanning mechanism for initiation of translation. *Gene*, **299**, 1–34.
36. Skabkin,M.A., Evdokimova,V., Thomas,A.A. and Ovchinnikov,L.P. (2001) The major messenger ribonucleoprotein particle protein p50 (YB-1) promotes nucleic acid strand annealing. *J. Biol. Chem.*, **276**, 44841–44847.
37. Kiang,J.G. and Tsokos,G.C. (1998) Heat shock protein 70 kDa: molecular biology, biochemistry and physiology. *Pharmacol. Ther.*, **80**, 183–201.
38. Klemenz,R., Hultmark,D. and Gehring,W.J. (1985) Selective translation of heat shock mRNA in *Drosophila melanogaster* depends on sequence information in the leader. *EMBO J.*, **4**, 2053–2060.
39. McGarry,T.J. and Lindquist,S. (1985) Cytoplasmic mRNA–protein interactions in eukaryotic gene expression. *Cell*, **42**, 903–911.
40. Bargou,R.C., Jurchott,K., Wagener,C., Bergmann,S., Metzner,S., Bommert,K., Mapara,M.Y., Winzer,K.J., Dietel,M., Dorken,B. and Royer,H.D. (1997) Nuclear localization and increased levels of transcription factor YB-1 in primary human breast cancers are associated with intrinsic MDR1 gene expression. *Nature Med.*, **3**, 447–450.
41. Oda,Y., Sakamoto,A., Shinohara,N., Ohga,T., Uchiumi,T., Kohno,K., Tsuneyoshi,M., Kuwano,M. and Iwamoto,Y. (1998) Nuclear expression of YB-1 protein correlates with P-glycoprotein expression in human osteosarcoma. *Clin. Cancer Res.*, **4**, 2273–2277.
42. Uramoto,H., Izumi,H., Ise,T., Tada,M., Uchiumi,T., Kuwano,M., Yasumoto,K., Funa,K. and Kohno,K. (2002) p73 Interacts with c-Myc to regulate Y-box-binding protein-1 expression. *J. Biol. Chem.*, **277**, 31694–31702.
43. Steel,L.F., Telly,D.L., Leonard,J., Rice,B.A., Monks,B. and Sawicki,J.A. (1996) Elements in the murine c-mos messenger RNA 5′-untranslated region repress translation of downstream coding sequences. *Cell Growth Differ.*, **7**, 1415–1424.
44. Kevil,C., Carter,P., Hu,B. and DeBenedetti,A. (1995) Translational enhancement of FGF-2 by eIF-4 factors and alternate utilization of CUG and AUG codons for translation initiation. *Oncogene*, **11**, 2339–2348.
45. Vagner,S., Gensac,M.C., Maret,A., Bayard,F., Amalric,F., Prats,H. and Prats,A.C. (1995) Alternative translation of human fibroblast growth factor 2 mRNA occurs by internal entry of ribosomes. *Mol. Cell. Biol.*, **15**, 35–44.
46. Bernstein,J., Shefler,I. and Elroy-Stein,O. (1995) The translational repression mediated by the platelet-derived growth factor 2/c-sis mRNA

leader is relieved during megakaryocytic differentiation. *J. Biol. Chem.*, **270**, 10559–10565.
47. Hengst,L. and Reed,S.I. (1996) Translational control of p27Kip1 accumulation during the cell cycle. *Science*, **271**, 1861–1864.
48. Sonenberg,N. (1993) Translation factors as effectors of cell growth and tumorigenesis. *Curr. Opin. Cell Biol.*, **5**, 955–960.
49. Miller,S.J., Suthiphongchai,T., Zambetti,G.P. and Ewen,M.E. (2000) p53 binds selectively to the 5′ untranslated region of cdk4, an RNA element necessary and sufficient for transforming growth factor beta- and p53-mediated translational inhibition of cdk4. *Mol. Cell. Biol.*, **20**, 8420–8431.

Cyclooxygenase 2 is a key enzyme for inflammatory cytokine-induced angiogenesis

TAKASHI KUWANO,* SHINTARO NAKAO,* HIDETAKA YAMAMOTO,† MASAZUMI TSUNEYOSHI,† TOMOYA YAMAMOTO,‡ MICHIHIKO KUWANO,§ AND MAYUMI ONO*,[1]

Departments of *Medical Biochemistry, †Anatomic Pathology, Pathological Sciences, and ‡Otorhinolaryngology, Graduate School of Medical Sciences, Kyushu University, Higashi-ku, Fukuoka 812-8582, Japan; and §Research Center for Innovative Cancer Therapy, Kurume University, Kurume, Fukuoka 830-0011, Japan

ABSTRACT **Cyclooxygenase1 (COX1) and COX2 mediate the rate-limiting step in arachidonic acid metabolism. Expression of COX2 mRNA and protein is often enhanced in various human cell types by inflammatory cytokines such as interleukin-1β (IL-1β) and tumor necrosis factor α (TNFα). IL-1β enhanced expression of various prostanoids and this expression was blocked by COX2 selective inhibitors. IL-1β markedly induced angiogenesis in vitro and in vivo, which was significantly inhibited by COX2 selective inhibitors but not by a vascular endothelial growth factor (VEGF) receptor tyrosine kinase inhibitor. In contrast, COX2 selective inhibitors only partially blocked VEGF-induced angiogenesis. EP2, EP4 (prostaglandin E2 receptors) agonists and thromboxane A2 (TXA2) receptor agonists induced angiogenesis in vitro and in vivo; IL-1β-induced angiogenesis was blocked by an EP4 antagonist and a TXA2 receptor antagonist. IL-1β induced much less angiogenesis in cornea of COX2 knockout mice than that of wild-type mice. This is the first report that COX2 and some prostanoids play a key role in IL-1β-induced angiogenesis.—Kuwano, T., Nakao, S., Yamamoto, H., Tsuneyoshi, M., Yamamoto, T., Kuwano, M., Ono, M. Cyclooxygenase 2 is a key enzyme for inflammatory cytokine-induced angiogenesis. *FASEB J.* 18, 300–310 (2004)**

Key Words: COX2 · vascular endothelial growth factor · prostanoid · inflammatory disease

BOTH ISOFORMS of cyclooxygenase (COX), constitutive COX1 and inducible COX2, catalyze the production of prostanoids from arachidonic acid (1). COX2-induced production of prostanoids is often implicated in inflammatory diseases, characterized by edema and tissue injury due to the release of many inflammatory cytokines and chemotactic factors, prostanoids, leukotrienes, and phospholipase (2, 3). Enhanced COX2-induced synthesis of prostaglandins stimulates cancer cell proliferation (4), promotes angiogenesis (5, 6), inhibits apoptosis (7), and increases metastatic potential (8). COX2 is also closely involved in the carcinogenesis process (9) and is overexpressed in adenocarcinoma in comparison with noncancerous mucosal regions in colon cancers (10) and gastric cancers (11). Elevated levels of mRNA and protein of COX2 are known to be associated with esophageal, head and neck, breast, lung, prostate, and other cancers, indicating a close involvement of COX2 in tumor progression and other pathological phenotypes in various malignant tumors (6, 9). COX2 is also known to be associated with lymph node metastasis in gastric cancer (12) and to affect the prognosis in primary lung adenocarcinoma (13).

On the other hand, ovulation is closely controlled by prostaglandins (14). Mice deficient in COX2 fail to ovulate, and this ovulatory failure could be restored by prostaglandin E2 (PGE2) or IL-1β and gonadotropins (15), suggesting that IL-1β/PGE2 plays a key role in ovulation. Numerous cytokines, hormones, growth factors, and chemical stimuli up-regulate expression of COX2 in various cell types including malignant cells, stromal cells, epithelial cells, and nonepithelial cells (9). Of these many stimuli, IL-1β has been well known to stimulate COX2 expression and/or PGE2 production in various cell types including monocytes/macrophages (16), vascular endothelial cells (17), colon fibroblasts (18), neuroblastoma cells (19), and osteoblasts (20). IL-1β-induced activation of the COX2 gene is modulated by various transcription factors such as NF-κB, IL-6, CRE (17, 21, 22). We have reported that potent angiogenic factors such as VEGF, IL-8, basic fibroblast growth factor (bFGF), metalloproteinases, and plasminogen activators are up-regulated in response to a representative inflammatory cytokine, TNFα in endothelial cells (23). In human cancer cells, IL-1α/β resulted in enhanced production of angiogenic factors VEGF and IL-8 (24). These findings led us to theorize that angiogenesis induced by TNFα and/or IL-1α/β is partially attributable to the production of such angiogenic factors (25). It remains unclear, how-

[1] Correspondence: Department of *Medical Biochemistry, Graduate School of Medical Sciences, Kyushu University, Maidashi 3-1-1, Higashi-ku, Fukuoka 812-8582, Japan. E-mail: mayumi@biochem1.med.kyushu-u.ac.jp

doi: 10.1096/fj.03-0473com

0892-6638/04/0018-0300 © FASEB

ever, whether representative inflammation-related substances such as prostanoids play any role in inflammatory angiogenesis.

A recent highlight is the development of COX2 inhibitors, known as nonsteroidal anti-inflammatory drugs (NSAIDs). Clinical trials of these NSAIDs have been performed for some inflammatory diseases such as rheumatoid arthritis and osteoarthritis (26, 27). NSAIDs have been shown to inhibit the growth of human colon tumor cells expressing higher levels of COX2 in vitro as well as in vivo (28). Treatment with NSAIDs decreased polyp number and size in familial adenomatous polyposis patients, indicating that NSAIDs may be chemopreventive against human polyposis (29). COX2 inhibitors markedly reduced polyposis in adenomatous polyposis coli (Apc) mice (30, 31), suggesting that selective COX2 inhibitors have potential as chemopreventive agents against human intestinal and colon cancer. One possible mechanism by which NSAIDs could modulate carcinogenesis, tumor growth, and other malignancy-related phenotypes in various tumors is their effects on tumor angiogenesis (9). Using animal models with Apc mutations during polyp formation, selective COX2 inhibitors decreased the expression of VEGF, a potent angiogenic factor (31). Overexpression of COX2 in colon cells is accompanied by up-regulation of VEGF, bFGF, nitric oxide synthases, and angiogenesis (6). COX2 inhibitors suppress both angiogenesis and tumor growth of xenografts of cancer cells in vivo (32). It was reported that a COX2 inhibitor suppressed angiogenesis induced by bFGF in rat corneas (33). Their studies suggest that NSAIDs may modulate tumor growth and carcinogenesis through antiangiogenesis. However, the underlying mechanism by which NSAIDs inhibit angiogenesis remains unclear. In our present study, we examine whether COX2 is directly associated with angiogenesis using various angiogenesis models and present a plausible model in which a COX2 inhibitor specifically induces antiangiogenic activity.

MATERIALS AND METHODS

Agents used

One COX2 inhibitor (DFU) was obtained from Banyu Pharmaceutical Co., Tokyo, and another (JTE-522) from Japan Tobacco Inc., Tokyo. The characteristics of these COX2 inhibitors were previously reported (34, 35). The chemical structures of DFU and JTE522 are shown in Fig. 1. ONO-AE1-259 (a PGE2 receptor EP2 agonist), ONO-AE1-329 (a PGE2 receptor EP4 agonist), ONO-AE3-208 (an EP4 antagonist), ONO-NT-126 (TXA2 receptor antagonists, used for in vitro), and ONO-8809 (orally active type of ONO-NT-126, used for in vivo) were obtained from ONO Pharmaceutical Co, Tokyo. U46619 (a TXA2 receptor agonist) was purchased from Cayman Chemical Co. (Ann Arbor, MI, USA). IL-1β and VEGF were purchased from R&D Inc. (Minneapolis, MN, USA).

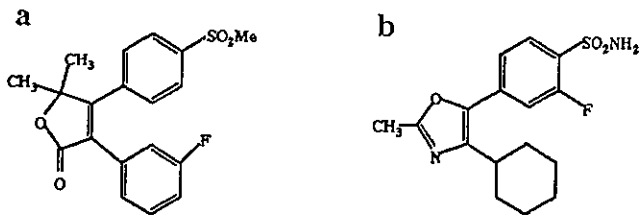

Figure 1. Chemical structures of COX2 inhibitors, DFU (*a*) and JTE522 (*b*). DFU and JTE522 are selective inhibitors of COX2 without significant activity on COX1. The chemical name of DFU ($C_{19}H_{17}FO_4S$; mol wt 360. 4) is 3-(3-fluorophenyl)-4(4-[methylsulfonyl] phenyl)-5, 5-dimethyl-5H-furan-2-one, and that of JTE522 ($C_{16}H_{19}FN_2O_3S$; mol wt 338. 4) is 4-(4-cyclohexyl-2-methyl-1, 3-oxazol-5-yl)-2-fluorobenzenesulfonamide.

Cell culture

HUVECs (Clonetics Inc., San Francisco, CA, USA) were cultured according to the manufacturer's instructions (36, 37).

Western blot analysis

Confluent KB3-1 cells were cultured in medium containing 2% NBS and HUVECs in medium containing 0.5% FBS for 24 h. The cells were then preincubated with COX2 inhibitors for 4 h before 1 ng/mL IL-1β or 20 ng/mL VEGF and incubated for 24 h at 37°C. Cells were then rinsed with ice-cold PBS and lysed in Triton X-100 buffer (50 μM HEPES, 150 μM NaCl, 1% Triton X-100, and 10% glycerol containing 1 μM PMSF, 1 mg/mL aprotinin, 1 mg/mL leupeptin, and 2 μM sodium vanadate). Cell lysates were subjected to SDS-PAGE and transferred to Immobilon membranes (Millipore, Bedford, MA, USA). After transfer, blots were incubated with the blocking solution and probed with anti-COX1 antibody, or anti-COX2 antibody, followed by washing. The protein content was visualized using HRP-conjugated secondary antibodies, followed by enhanced chemiluminescence (ECL, Amersham).

Migration assay of HUVECs

This assay was performed using a multiwell chamber. Polycarbonate filters (8 μm pores) were coated with 1.33 μg/mL fibronectin for 1 h at 37°C and used as the inner chamber (36, 37). HUVECs (3×10^5 cells) were suspended in EBM containing 0.5% FBS and seeded into the inner chamber. In the outer chamber, we added an EP4 agonist (ONO-AE1-329, 1 or 10 μM), a TXA2 receptor agonist (U46619, 1 or 10 μM), PGF2 (1 or 10 μM). VEGF (20 ng/mL), or IL-1β (1 ng/mL), with or without serial dilutions of DFU (10 or 100 μM) or JTE522 (10 or 100 μM). IL-1β, with or without EP4 antagonist (ONO-AE3-208, 1 or 10 μM) or TXA2 receptor antagonist (ONO-NT-126, 1 or 10 μM) in the same medium, was added. After incubation for 5 h at 37°C, nonmigrated cells on the upper surface of the filter were removed and cells that had migrated under the filter were counted. Cells were counted using average numbers from assays of three chambers.

Corneal micropocket assay in mice and quantification of corneal neovascularization

The corneal micropocket assay in mice has been described (36, 37). Briefly, 0.3 μL of hydron pellets (IFN Sciences, New

Brunswick, NJ, USA) containing IL-1β (30 ng/pellet), the EP2 agonist ONO-AE1-259 (1 or 10 μg/pellet), the EP4 agonist ONO-AE1-329 (1 or 10 μg/pellet), the TXA2 receptor agonist U46619 (50 or 100 μg/pellet), PGF2 (50 or 100 μg/pellet), or VEGF (200 ng/pellet) was prepared and implanted in the corneas of male BALB/c mice. DFU (50 mg · kg^{-1} · day^{-1}), JTE522 (50 or 100 mg · kg^{-1} · day^{-1}), the EP4 antagonist ONO-AE3-208 (1 mg · kg^{-1} · day^{-1}), and the TXA2 receptor antagonist ONO-8809 (1 mg · kg^{-1} · day^{-1}) were administered orally on days 1–6, and the VEGF receptor tyrosine kinase inhibitor SU5416 was administered intraperitoneally on days 1–6. On day 6, the mice were killed and their corneal vessels were photographed. Images of the corneas were recorded using Nikon Coolscan software. Areas of corneal neovascularization were analyzed using the software package NIH Image 1.61 (36, 37) and expressed in mm^2. The corneal micropocket assay was also performed with COX2 knockout mice. COX2 knockout mice (C57BL/6, 129P2-Ptgs2 ^{tm1Smi}) (38) were purchased from Taconic Farms Inc. (Germantown, NY, USA). In this assay, 0.3 μL of hydron pellets containing IL-1β (30 ng/pellet) or VEGF (200 ng/pellet) were implanted in the corneas of male COX2 knockout or wild-type mice. As wild-type counterpart, C57 Black mouse was used.

ELISA assays of PGE2 and TXA2/TXB2

Concentrations of PGE2 and TXA2/TXB2 in the condition medium of HUVECs were measured using commercially available ELISA kits. Cells were plated in 24-well dishes in medium containing 2% FBS. When cells were subconfluent, the medium was replaced with 0.5% serum medium for 24 h. The cells were then preincubated with various concentrations of DFU or JTE522 for 4 h, followed by 1 ng/mL IL-1β at 37°C. Assays were performed after 24 h of incubation with 0.5% serum medium. Results were normalized for the number of cells and reported as picograms of growth factor/10^4 cells/24 h.

Immunohistochemistry of mouse cornea

After stimulation by IL-1β for 6 days, cornea of Balb/cN mouse was formalin-fixed, paraffin-embedded, and sliced into sections (4 μm thick) as described (39). Tissue sections were immunohistochemically stained using polyclonal primary antibody and the Streptavidin-biotin-peroxidase method (Histofine SABPO Kit; Nichirei, Tokyo, Japan). COX2 polyclonal antibody (Dilution 1:200; Cayman) was used as a primary antibody.

RESULTS

Enhanced expression of COX2 by IL-1β and effect of COX2 inhibitors

A representative inflammatory cytokine, IL-1β, induces up-regulation of COX2 in various cell types. Western blot analysis was performed with specific antibodies against COX1 and COX2 to examine expression of both isoforms in human head and neck cancer KB3-1 cells and HUVECs. In KB3-1 cells and HUVECs, IL-1β did not enhance COX1 protein expression, indicating a constitutive expression of COX1 gene (Fig. 2*a*). Two COX2 inhibitors, DFU and JTE522, also had no effect on expression of COX1 protein. In contrast, there marked increases appeared in COX2 levels in KB3-1 cells as well as HUVECs by IL-1β. However, two COX2 inhibitors, DFU and JTE522, up to 50 μM did not block IL-1β-induced up-regulation of COX2 protein (Fig. 2*b*). Other inflammatory cytokines such as TNFα and IL-1α also enhanced production of COX2 protein but not that of COX1 (data not shown). IL-1β potently up-regulated expression of COX2 in various cell types used in this study. In contrast, VEGF, a representative angiogenic factor, did not enhance COX2 protein expression (Fig. 2*c*).

Production of prostanoids by IL-1β and effect of COX2 inhibitors

We first investigated whether IL-1β could enhance the production of prostanoids through the up-regulation of COX2 gene. HUVECs produce little if any prostanoids without the exogenous addition of cytokines (**Table 1**). IL-1β, however, induced marked production of prostanoids, including PGE2 and TXB2/TXA2. As TXA2 is very unstable, we therefore measured TXB2 (a relatively stable prostanoids derived from TXA2). Cellular production of both PGE2 and TXB2 was increased ~10-fold over the control by IL-1β alone. This IL-1β-induced production of these prostanoids was markedly inhibited by the addition of DFU or JTE-522 (Table 1). These two COX2 inhibitors were found to inhibit the production of prostanoids at similar dosages as used in this study when human cancer cells or monocytic cells were treated with IL-1β (data not shown).

Cell migration by vascular endothelial cells in response to IL-1β or prostanoids and effect of COX2 inhibitors

Cell migration of vascular endothelial cells is a key step in the process of neovascularization. We first examined whether IL-1β or prostanoids could stimulate cell migration and whether COX2 inhibitors could affect the IL-1β-induced migration of vascular endothelial cells. IL-1β at 1 ng/mL stimulated cell migration ~2.5-fold higher than the control, whereas VEGF at 20 ng/mL stimulated cell migration ~3.5-fold higher (Fig. 3*a*). DFU or JTE522 at a concentration of 100 μM resulted in marked inhibition of IL-1β-induced migration by vascular endothelial cells (Fig. 3*a*). In contrast, there was no evidence of inhibition by DFU or JTE52 at 100 μM on cell migration stimulated by VEGF (Fig. 3*a*). Exogenous addition of a PGE2 receptor EP2 agonist (ONO-AE1-259), EP4 agonist (ONO-AE1-329), or a TXA2 receptor agonist (U46619) at a concentration of 10 μM stimulated cell migration ~twofold over the control (Fig. 3*b*). There was, however, no apparent stimulation of cell migration by PGF2 (data not shown). The stimulatory effects of prostanoids were comparable to those of VEGF or IL-1β, and their stimulatory effects on cell migration were reproducibly observed. We then investigated which prostanoid was responsible for IL-1β-induced angiogenesis in vitro. IL-1β-induced cell

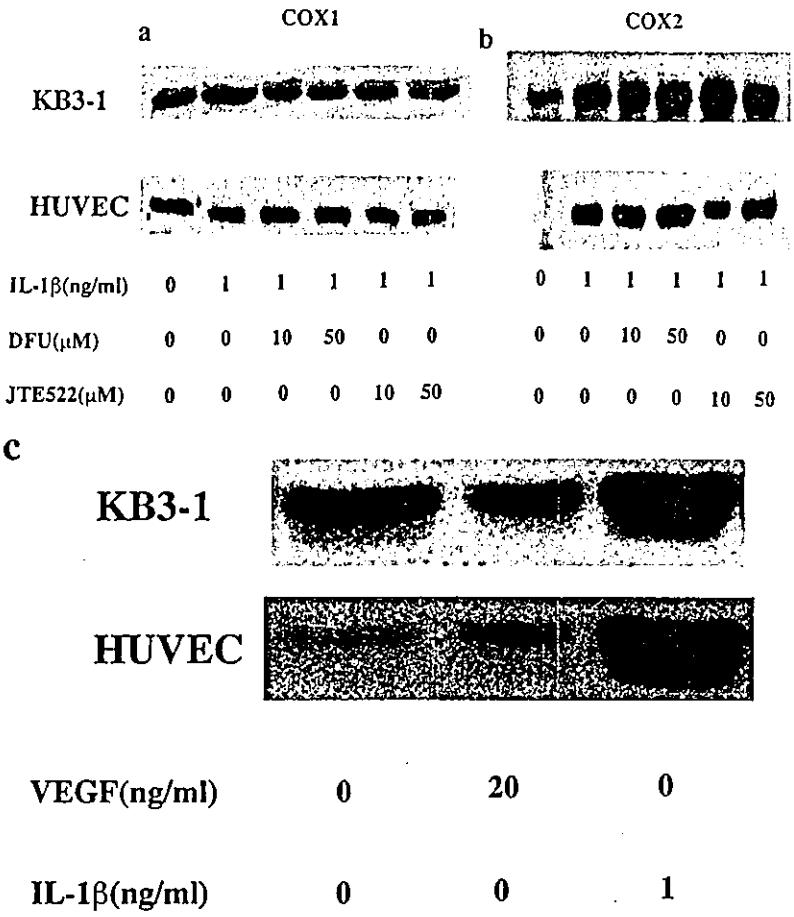

Figure 2. Effect of COX2 inhibitors on expression of COX1 and COX2 protein. Effects of COX2 inhibitors on protein expression of COX1 and COX2 protein in KB3-1 and HUVECs were compared by Western blot analysis. KB3-1 cells and HUVECs were incubated in the absence or presence of 1 ng/mL IL-1β with or without indicated doses of DFU or JTE522. The same amount of cellular protein was separated by SDS-PAGE and Western blot analysis was performed with specific antibody against COX1 (*a*) and COX2 (*b*). *c)* Protein levels of COX2 in KB3-1 cells and HUVECs were also compared when exposed to 20 ng/mL VEGF or 1 ng/mL IL-1β.

migration was significantly inhibited by an EP4 antagonist (ONO-AE3-208, 10 μM) and a TXA2 receptor antagonist (ONO-NT-126, 10 μM) (Fig. 3*c*). These findings suggest that COX2 activity is closely associated with IL-1β-induced angiogenesis in vitro. Moreover, TXA2 and PGE2 appeared to play critical roles in IL-1β-induced angiogenic activity in vitro.

TABLE 1. *IL-1β-induced production of prostanoids by vascular endothelial cells and inhibition of COX2 inhibitors*[a]

IL-1β (ng/mL)	COX2 inhibitor (μM)	PGE2 (pg/mL · 10^4 cells)	TXB2/TXA2 (pg/mL · 10^4 cells)
0	None	1.4	1.2
1	None	15.2 (100)[b]	15.8 (100)
1	DFU (0.3)	6.1 (34)	10.1 (61)
1	DFU (3.0)	4.8 (25)	5.9 (32)
1	DFU (30)	2.1 (5)	1.8 (4)
1	JTE522 (0.1)	6.9 (40)	10.5 (64)
1	JTE522 (1.0)	2.8 (10)	6.5 (35)
1	JTE522 (50)	2.4 (4)	2.0 (6)

[a] PGE2 and TXB2/TXA2 production into culture medium was measured by ELISA when HUVECs were stimulated with IL-1β and incubated with or without DFU or JTE522 for 24 h. [b] Each value (pg/mL · 10^4 cells/24 h) was the mean of duplicate cultures. In parentheses, IL-1β-induced production of prostanoids was recorded as 100% when cellular amounts of eicosanoids in the absence of the cytokine was subtracted from that in the presence of the cytokine alone.

Angiogenesis in vivo in response to IL-1β and the effect of selective COX2 inhibitors

We investigated whether IL-1β could induce angiogenesis in vivo in mouse corneas. Implantation of IL-1β at doses of 10–30 ng into mouse corneas was found to induce neovascularization in a nonvascular area of the cornea at rates comparable to 200 ng of VEGF. Apparent angiogenesis in the cornea in mice when either IL-1β at 30 ng or VEGF at 200 ng was implanted (Fig. 4*b, f*). Oral administration of DFU (50 mg · kg^{-1} · day^{-1}) or JTE522 (100 mg · kg^{-1} · day^{-1}) dramatically inhibited IL-1β-induced angiogenesis (Fig. 4*c, d*) but not VEGF-induced angiogenesis (Fig. 4*h*). In contrast, intraperitoneal administration of SU5416, a specific inhibitor of both VEGF receptors, KDR/Flk-1 and Flt-1 (40), almost completely inhibited VEGF-induced angiogenesis (Fig. 4*g*) but had no effect on IL-1β-induced angiogenesis in vivo (Fig. 4*e*). Quantitative analysis using three or four mice for each assay showed almost complete inhibition of IL-1β-induced neovascularization when DFU or JTE-522 was orally administered (Fig. 4*i*). Almost no inhibition by DFU (Fig. 4*h, i*) or JTE-522 (data not shown) of VEGF-induced neovascularization was observed, whereas SU5416 significantly inhibited VEGF-induced neovascularization. IL-1β-induced angiogenesis was blocked by selective COX2 inhibitors in vitro and in vivo.

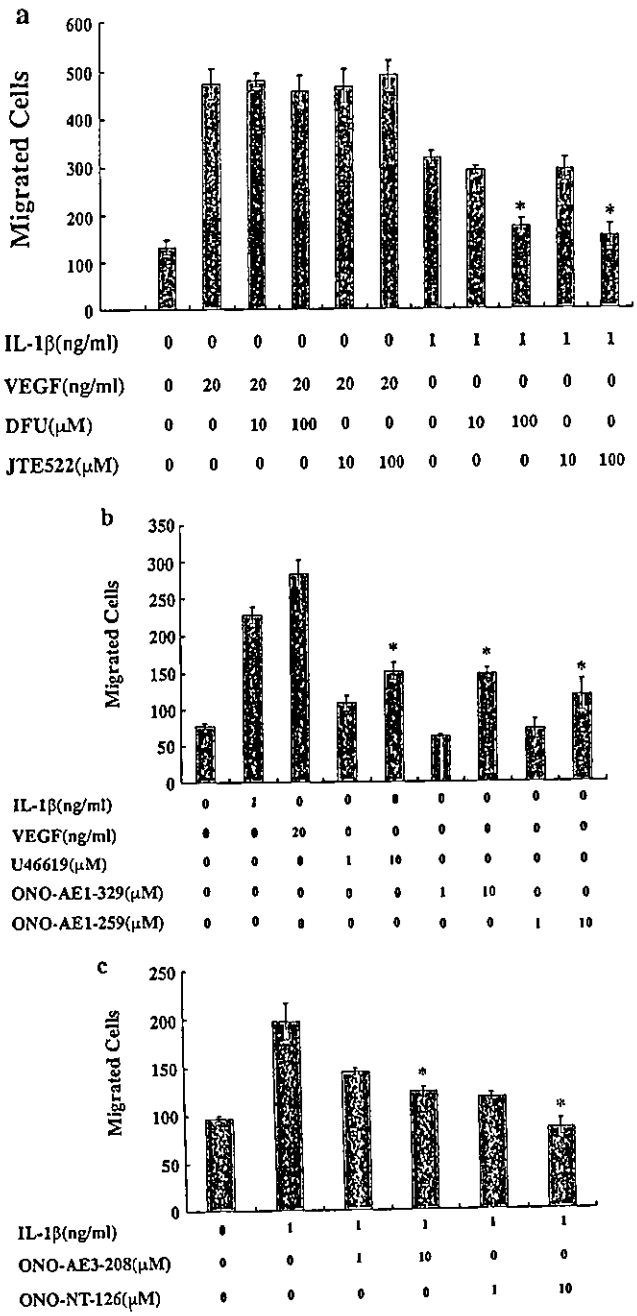

Figure 3. Effects of COX2 inhibitors and prostanoids on cell migration. *a)* Effects of COX2 inhibitors on endothelial cell migration by VEGF and IL-1β were assayed using HUVECs in vitro. The migrated cell number was the mean of triplicate dishes. Relative activity (%) was recorded as 100% when the cell number (133±9.7) in the absence of any factor was subtracted from that in the presence of VEGF (20 ng/mL) or IL-1β (1 ng/mL) alone. *b)* Effects of a TXA2 receptor agonist (U46619, 1 or 10 μM), a PGE2 receptor EP2 agonist (ONO-AE1-259, 1 or 10 μM) and EP4 agonist (ONO-AE1-329, 1 or 10 μM) on cell migration were determined by using HUVECs. *c)* Effects of a TXA2 receptor antagonist (ONO-NT-126) and an EP4 antagonist (ONO-AE3-208) on IL-1β-induced vascular endothelial cell migration. Both agents were found to significantly inhibit IL-1β-induced cell migration in vitro. Each column gives the average value ±SD when 3 independent assays were performed. *Statistically significant difference ($P<0.01$) to value for IL-1β alone.

Angiogenesis in vivo by prostanoid receptor agonists

We next investigated whether prostanoids could also induce neovascularization in mouse corneas in vivo. Corneal implantation of a TXA2 receptor agonist (U46619, 50 or 100 μg), an EP2 receptor agonist (ONO-AE1-259, 1 or 10 μg) or an EP4 receptor agonist (ONO-AE1-329, 1 or 10 μg) as a pellet was found to induce angiogenesis, although its neovascularization activity was less than that of IL-1β (Fig. 5*c–e*). In contrast, PGF2 did not induce angiogenesis (data not shown). Quantitative analysis using three or four mice for each assay showed angiogenic activity of TXA2 and PGE2 when their respective agonists were implanted (Fig. 5*f*).

Effect of prostanoid receptor antagonists on angiogenesis in vivo by IL-1β

We further investigated which prostanoid was most closely involved in IL-1β-induced angiogenesis. Oral administration of the TXA2 receptor antagonist ONO-8809 (1 mg · kg^{-1} · day^{-1}) or the EP4 receptor antagonist ONO-AE3-208 (1 mg · kg^{-1} · day^{-1}) was found to reduce IL-1β-induced angiogenesis in mouse corneas (Fig. 6*a–c*). Quantitative analysis showed that ONO-8809 and ONO-AE3-208 both significantly inhibited IL-1β-induced angiogenesis by ~50% (Fig. 6*d*).

Localization of COX2 in infiltrating cells within IL-1β–treated corneas

We examined whether COX2-positive cells were infiltrated in IL-1β-treated corneas. The cornea developed new vessels by IL-1β, immunohistochemical analysis of the corneas was performed with anti-COX2 antibody. Many infiltrating cells stained with COX2 appeared in the stroma and anterior chamber when treated with IL-1β (Fig. 7). By contrast, there appeared to be no infiltrating cells within the untreated corneas (data not shown). Cells infiltrated near new vessels in the cornea consisted of inflammatory cells, including monocyte/macrophage. Immunohistochemical analysis with murine macrophage-recognizing monoclonal antibody (F4/80) showed many F4/80-positive cells in IL-1β-treated cornea (data not shown).

Angiogenesis by IL-1β in COX2 knockout mice

We finally asked whether COX2 was directly involved in IL-1β-induced angiogenesis in vivo. We compared angiogenesis by IL-1β between COX2 knockout mice and wild-type mice. Implantation of IL-1β at a dose of 30 ng into cornea of wild-type mouse induced neovascularization in a nonvascular area. By contrast, a marked reduction in the angiogenesis in cornea of COX2 knockout mice was demonstrated (Fig. 8*b*). We observed angiogenesis at similar levels between wild-type and COX2 knockout mice by VEGF at a dose of 200 ng (Fig. 8*c, d*). Quantitative analysis using three to four

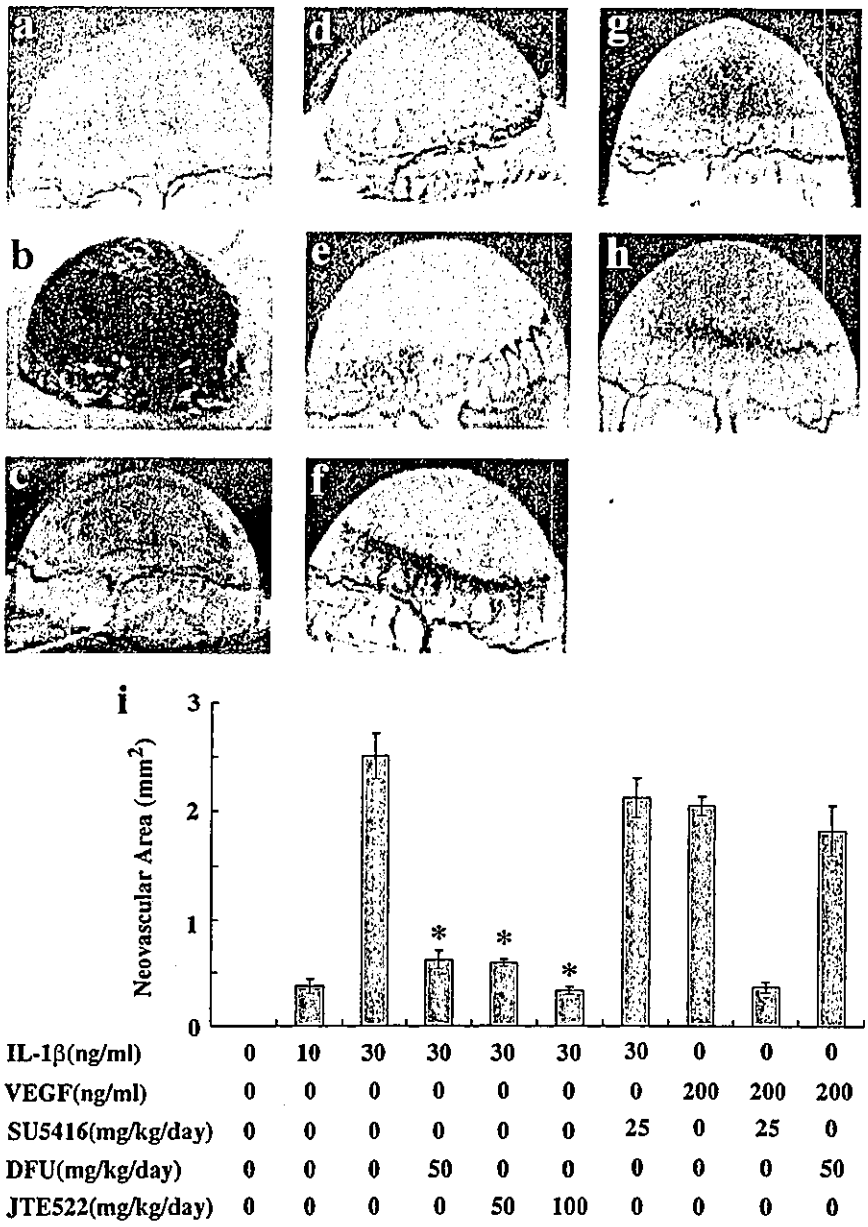

Figure 4. Effects of COX2 inhibitors on angiogenesis in vivo. Photographs of angiogenesis in mouse corneas. Mice were treated with DFU (50 mg · kg^{-1} · day^{-1}, orally), JTE522 (50 or 100 mg · kg^{-1} · day^{-1}, orally), or SU5416 (25 mg · kg^{-1} · day^{-1}, intraperitoneally) on day 1 to 6. Six days later, vessels in the region of the pellet implant were photographed. Representative photographs of mouse corneas; *a)* buffer alone, *b)* IL-1β (30 ng), *c)* IL-1β with DFU (50 mg · kg^{-1} · day^{-1}), *d)* IL-1β with JTE522 (100 mg · kg^{-1} · day^{-1}), *e)* IL-1β with SU5416 (25 mg · kg^{-1} · day^{-1}), *f)* VEGF (200 ng), *g)* VEGF with SU5416 (25 mg · kg^{-1} · day^{-1}), *h)* VEGF with DFU (50 mg · kg^{-1} · day^{-1}). *i)* Quantification of corneal neovascularization in mice after administration of DFU, JTE522, or SU5416. Neovascular areas developed in mouse corneas (*a–h*) were quantified as described in Materials and Methods. Columns are mean (±SD) of 3 or 4 independent experiments. *Statistically significant difference ($P<0.01$) to value for IL-1β alone.

mice for each assay showed very low (~20%) angiogenesis by IL-1β in COX2 knockout mice in comparison with wild-type mice (Fig. 8*e*). A similar level of angiogenic activity in vivo by VEGF between COX2 knockout and wild-type mice was observed (Fig. 8*e*).

DISCUSSION

Voronov et al. recently reported that IL-1 is required for both angiogenesis and tumor invasiveness using IL-1β or IL-1α knockout mice (41). Other independent studies have reported that IL-1β promotes tumor growth, invasion, and angiogenesis in animal models with concomitant enhanced production of VEGF, MMP-2, IL-8, and adhesion molecules (42, 43). IL-1α also promotes angiogenesis in vivo through VEGF receptor pathway possibly by inducing VEGF synthesis (44). However, it remains unclear how VEGF or other angiogenesis-related factors could be involved in IL-1-induced angiogenesis and tumor invasion. In our present study, IL-1β was found to markedly enhance production of prostanoids such as PGE2 and TXA2/TXB2. IL-1β-induced production of prostanoids was almost completely blocked by both COX2-selective inhibitors DFU and JTE522. Both cell migration by vascular endothelial cells in vitro and corneal neovascularization in vivo were markedly induced in response to IL-1β at rates similar to VEGF. Administration of COX2 inhibitors resulted in a dramatic reduction of IL-1β-induced angiogenesis in vivo as well as cell migration in vitro. A TXA2 receptor agonist (U46619), an EP2 agonist (ONO-AE1-259), and an EP4 agonist (ONO-AE1-329) stimulated cell migration in vitro and induce corneal neovascularization in mice. TXA2 receptor antagonists (ONO-8809) and EP4 antagonist

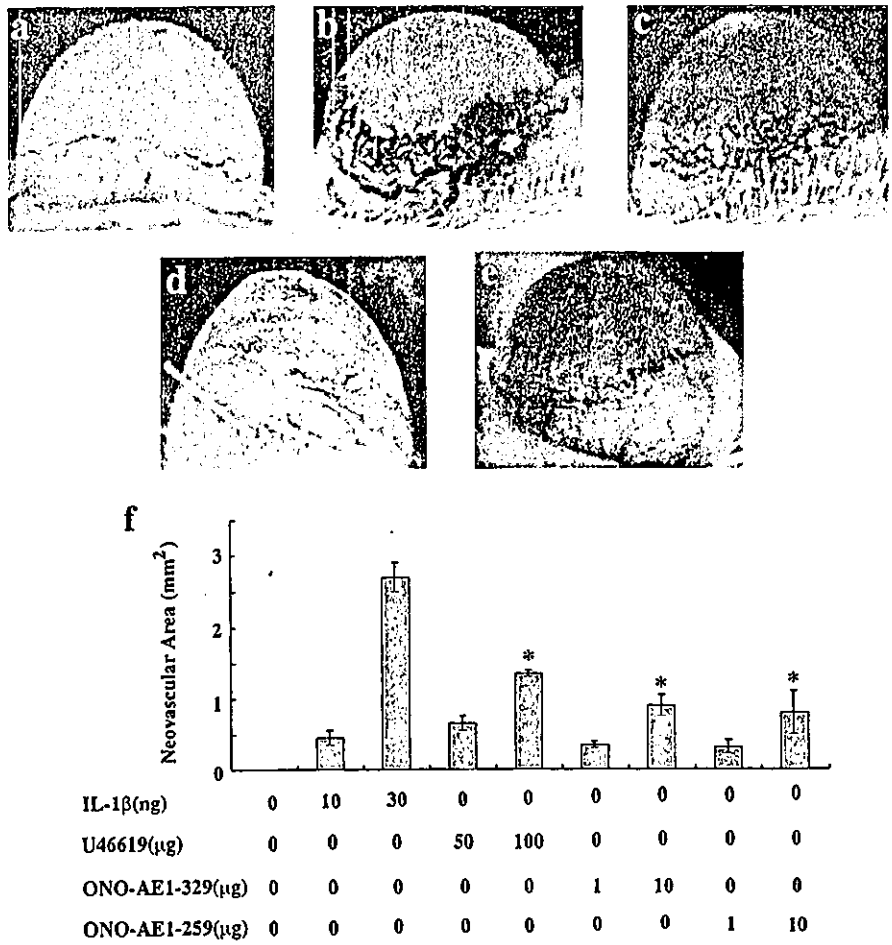

Figure 5. Angiogenesis in vivo by prostanoid receptor agonists. Photographs of angiogenesis in mouse corneas. Hydron pellets containing of *a)* buffer alone, *b)* IL-1β (30 ng/pellet), *c)* TXA2 receptor agonist (U46619, 100 μg/pellet), *d)* EP2 agonist (ONO-AE1-259, 10 μg/pellet), *e)* EP4 agonist (ONO-AE1-329, 10 μg/pellet) were implanted into the corneas of Balb/c mice. Six days later vessels in the region of the pellet implanted were photographed. Quantitative analysis was performed on data in panel *f* with 3 or 4 mice corneas.

(ONO-AE3-208) also inhibited IL-1β-induced angiogenesis in vivo. We therefore present a model that some prostanoids such as TXA2 and PGE2 directly induce angiogenesis through interaction with their cognate receptors on vascular endothelial cells (Fig. 9).

We also observed apparent reduction in IL-1β-induced angiogenesis in corneas of the COX2 knockout mice in comparison with wild-type mice. This experiment with knockout mice strongly suggests a direct involvement of COX2 and relevant prostanoids in

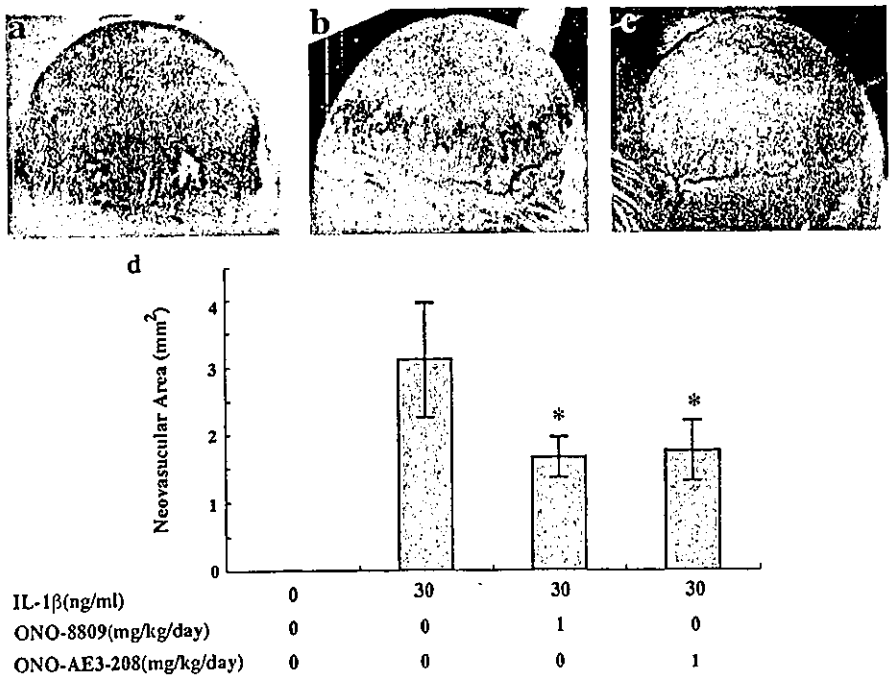

Figure 6. Inhibition of IL-1β–induced angiogenesis by prostanoid receptor antagonists. Photographs of angiogenesis in mouse corneas. Hydron pellets containing IL-1β (30 ng/pellet) were implanted into the corneas of Balb/c mice. TXA2 receptor antagonist (ONO-8809, 1 mg · kg^{-1} · day^{-1}) or the PGE2 receptor EP4 antagonist (ONO-AE3-208, 1 mg · kg^{-1} · day^{-1}) was administered orally on day 1 to 6. Representative photographs of mouse corneas *a)* IL-1β (30 ng/pellet), *b)* IL-1β with ONO-8809 (1 mg · kg^{-1} · day^{-1}), and *c)* IL-1β with ONO-AE3-208 (1 mg · kg^{-1} · day^{-1}). *d)* Quantitative analysis was performed on data in panels *a–c* with 3 or 4 mice corneas. *Statistically significant difference ($P<0.01$) to value for IL-1β alone.

Figure 7. Identification of COX2-positive cells infiltrating in corneas treated with IL-1β. Immunohistochemical staining was preformed with the sections of IL-1β-treated cornea in mice with anti-COX2 antibody (*a, b*). The black arrows represent new vessels and the red arrows represent COX2 positive cells. Compared with untreated group (data not shown), section of IL-1β-treated corneas shows numerous immunopositive cells in stroma and anterior chamber. Magnification, 40× (*a*), 100× (*b*).

IL-1β-induced angiogenesis. However, some neovascularized area was observed in the COX2 knockout mice by IL-1β, suggesting an involvement of different factors or pathways in IL-1β-induced angiogenesis.

COX2 overexpresssion up-regulates expression of several angiogenic factors, VEGF and bFGF, and COX2 inhibitors significantly inhibited production of VEGF and bFGF as well as angiogenesis in vivo (32, 45). Administration of COX2 inhibitors blocked expression of VEGF and bFGF in vitro as well as angiogenesis and tumor growth in vivo (32). It has been reported that prostaglandins stimulate production of VEGF and bFGF (46). We have reported that IL-1α and TNFα significantly enhance production of VEGF, IL-8, bFGF (23, 24), and COX2 protein in endothelial cells and cancer cells (Fig. 9). Such potent angiogenic factors are expected to be involved in angiogenesis through the IL-1α/β-COX2 pathway (17). It seems likely there are at least two pathways in the IL-1β-induced production of VEGF and other factors through either COX2-dependent or COX2-independent pathways. IL-1β-induced production of VEGF and IL-8 was, however, inhibited by only ~50% when treated with COX2 inhibitors at concentrations of 50 to 100 μM (T. Kuwano and M. Ono, unpublished data). In contrast, COX2 inhibitors at low concentrations markedly inhibited IL-1β-induced production of PGE2 and TXB2/TXA2 (Table 1). Our in vivo study further demonstrated that IL-1β-induced corneal angiogenesis in vivo was blocked, but not completely, by DFU and JTE522. This IL-1β-induced angiogenesis was blocked only slightly if at all by SU5416. This in vivo study suggests specific involvement of prostanoids in IL-1β-induced angiogenesis rather than in angiogenesis by the VEGF/VEGF receptor pathway (Fig. 9).

Arachidonic acid metabolites have been known to modulate endothelial cell proliferation or migration

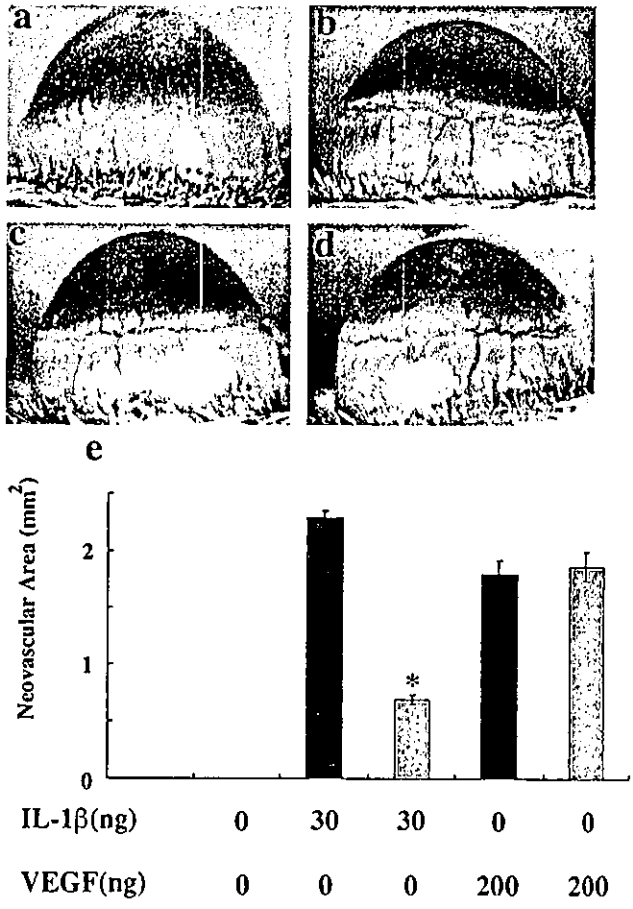

Figure 8. Angiogenesis in cornea of COX2 knockout mice Photographs of angiogenesis in mouse corneas. IL-1β or VEGF was implanted in corneas of COX2 knockout mice and wild-type mice on day 1. Six days later, vessels in the region of the pellet implanted were photographed. Representative photographs of angiogenesis in corneas of wild-type and COX2 knockout mice *a)* wild-type mouse: IL-1β (30 ng); *b)* COX2 knockout mouse: IL-1β (30 ng); wild-type mouse: VEGF (200 ng); and *d)* COX2 knockout mouse: VEGF (200 ng). *e)* Quantitative analysis was performed on data in panels *a–d* with 3 or 4 mice corneas. Black bars represent wild-type mice; blue bars represent COX2 knockout mice. *Statistically significant difference ($P<0.01$) to the value for IL-1β in wild-type mouse.

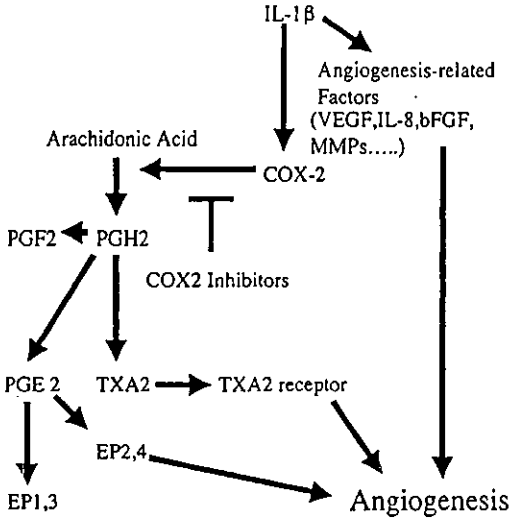

Figure 9. A model for IL-1β-induced angiogenesis and effect of COX2 inhibitor. We previously reported that IL-1β and TNF-α enhance production of angiogenesis-related factors such as VEGF, IL-8, bFGF, plasminogen activator, and metalloproteinases from vascular endothelial cells and other cell types, resulting in angiogenesis through autocrine and/or paracrine control. In the present study, we demonstrated that inflammatory cytokines such as IL-1β and probably TNF-α induce angiogenesis through the direct interaction of prostanoids with vascular endothelial cells. COX2 induced by IL-1β catalyzes the process of arachidonic acid cascade in vascular endothelial cells. PGE2 and TXA2 are prostanoids, final products of the arachidonic acid cascade thought to be critical factors for angiogenesis through PGE2 receptors (EP2, EP4) and the TXA2 receptor.

and capillary formation in vivo (47). We previously reported that arachidonic acid metabolism inhibitors block angiogenesis in vivo as well as in vitro, suggesting a close association between prostanoids and angiogenesis. Of the various prostanoids produced by COX2 in response to IL-1β, PGE2 appears to play a key role in inflammatory angiogenesis (5). PGI2 (48) and TXA2 (49) were reported to demonstrate some angiogenic activity in vivo. Our study indicated that PGE2 and TXA2 stimulate cell migration by vascular endothelial cells. Cell migration in response to IL-1β, but not to VEGF, was blocked by DFU or JTE522. Angiogenesis assay in vivo also demonstrated induction of angiogenesis in corneas by a TXA2 receptor agonist (U46619) and an EP4 agonist (ONO-AE-329). Taken together, these results consistently support the notion that inflammatory cytokine-elicited angiogenesis is induced mainly by TXA2, PGE2, and other undetermined prostanoids through COX2 activation. Both COX2 inhibitors at low concentrations significantly inhibited the production of PGE2 and TXA2/TXB2 whereas at high concentrations inhibited the IL-1β-induced migration of vascular endothelial cells (Table1 and Fig. 3). Concerning this discrepancy, experimental conditions for the two assay systems are different. *1)* In the migration assay, IL-1β and COX2 inhibitors were added simultaneously while COX2 inhibitors were added 4 h before exposure to IL-1β in the prostanoid production assay. *2)* Migration assay was performed for only 5 h whereas prostanoid production assay was performed for 24 h. We still favor the idea that PGE2 and TXA2/TXB2 play key roles in IL-1β-induced cell migration. However, further study is required to determine the involvement of prostanoids other than PGE2 and TXA2/TXB2 and/or angiogenic factors in the IL-1β-induced cell migration.

The tumor microenvironment consists mainly of various inflammatory cells and closely affects proliferation, survival and migration in the neoplastic process (50). Of these inflammatory cell types, macrophage is a significant component of inflammatory infiltrates, affecting angiogenesis as well as malignant characteristics of cancer. Infiltration of macrophages is closely associated with microvascular density and malignant status in various human tumor types (24). Activated macrophages are thought to play a key role in angiogenesis of inflammatory diseases and in malignant tumors. Activated macrophages infiltrating tumor stroma and inflammatory regions produce various angiogenesis factors, including prostanoids (25). Related studies have reported that activation of macrophage is accompanied by induction of COX2 and IL-1β (16) and that high expression of COX2 is often observed in macrophages infiltrating in tumor stroma (18). We have reported that macrophage infiltration is maximized in mouse cornea within 4 to 5 days after inflammatory stimuli by chemical cauterization and that the kinetics of macrophage infiltration is similar to that of neovascularization (39). Consistent with this study, inflammatory cytokine IL-1β could induce infiltration of COX2-positive macrophages and/or other inflammatory cells in cornea. If such macrophages/monocytes actively produce prostanoids, these prostanoids could also play a key role in angiogenesis under certain inflammatory conditions.

NSAIDs block tumor development in some animal carcinogenesis models (30). In a recent study, COX2 overexpression in the skin of transgenic mice resulted in suppression of tumor development, again suggesting a key role for COX2 and elevated prostaglandin levels in the development of skin tumor (51). On the other hand, angiogenesis, a risk factor for metastasis and recurrence (52), is closely involved in the tumor development process. Angiogenesis is a prerequisite for the early switch-on of tumor development in several animal carcinogenesis models. Anticarcinogenic and antineoplastic effects of NSAIDs are known to be mediated through COX2-dependent and -independent pathways (53). Anticarcinogenesis and antineoplastic effects through inhibition of COX2 dependent pathways could be attributable at least in part to inhibition of angiogenesis by NSAIDs. The clinical application of COX2 inhibitors will provide new information as to whether COX2 is a useful molecular target. FJ

We would like to thank Banyu Pharmaceutical Co. and Japan Tobacco Inc. for COX2 inhibitors and ONO Pharmaceutical Co. for prostanoid receptor agonists and antagonists. This work was supported by grants for cancer research from the Ministry of Education, Science, Sport and Culture, Japan (M.O., M.K.), and the Ministry of Human Health Labor and Welfare, Japan (M.K.).